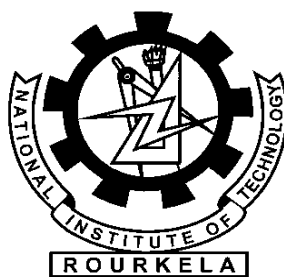


Three Dimensional Analysis of Combined Extrusion-forging Process

**A THESIS SUBMITTED IN PARTIAL FULFILLMENT OF
THE REQUIREMENT FOR THE AWARD OF THE DEGREE
OF
MASTER OF TECHNOLOGY
IN
MECHANICAL ENGINEERING
(SPECIALIZATION IN PRODUCTION ENGINEERING)
BY
KANHU CHARAN NAYAK
(ROLL NO. 211ME2352)**



**NATIONAL INSTITUTE OF TECHNOLOGY ROURKELA
ROURKELA-769008, INDIA**

Three Dimensional Analysis of Combined Extrusion-forging Process

A THESIS SUBMITTED IN PARTIAL FULFILLMENT OF
THE REQUIREMENT FOR THE AWARD OF THE DEGREE
OF

MASTER OF TECHNOLOGY

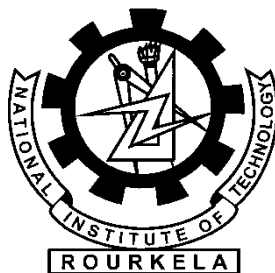
IN
MECHANICAL ENGINEERING
(SPECIALIZATION IN PRODUCTION ENGINEERING)

BY
KANHU CHARAN NAYAK

(ROLL NO. 211ME2352)

Under the Guidance of

Prof. Susanta Kumar Sahoo
Department of Mechanical Engineering



NATIONAL INSTITUTE OF TECHNOLOGY ROURKELA
ROURKELA-769008, INDIA

2013



Department of Mechanical Engineering
National Institute of Technology
Rourkela

CERTIFICATE

This to certify that the thesis entitled “**Three Dimensional Analysis of Combined Extrusion-forging Process**” being submitted by **Kanhu Charan Nayak** for the award of the degree of Master of Technology (Production Engineering) of NIT Rourkela, is a record of bonafide research work carried out by him under my supervision and guidance. Mr. Kanuh Charan Nayak has worked for more than one year on the above problem at the Department of Mechanical Engineering, National Institute of Technology, Rourkela and this has reached the standard fulfilling the requirements and the regulation relating to the degree. The contents of this thesis, in full or part, have not been submitted to any other university or institution for the award of any degree or diploma.

Place: Rourkela
Date:

Prof. Susanta Kumar Sahoo
(Supervisor)
Professor
Department of Mechanical Engineering
NIT, Rourkela-769008

ACKNOWLEDGEMENT

This thesis is a result of research that has been carried out at **National Institute of Technology, Rourkela**. During this period, I came across with a great number of people whose contributions in various ways helped my field of research and they deserve special thanks. It is a pleasure to convey my gratitude to all of them.

In the first place, I would like to express my deep sense of gratitude and indebtedness to my supervisors **Prof. S.K. Sahoo** for his advice, and guidance from early stage of this research and providing me extraordinary experiences throughout the work. Above all, he provided me unflinching encouragement and support in various ways which exceptionally inspire and enrich my growth as a student, a researcher. His involvement with originality has triggered and nourished my intellectual maturity that will help me for a long time to come. I am proud to record that I had opportunity to work with an exceptionally experienced scientist like him.

I am grateful to Director, **Prof. S.K. Sarangi**, and **Prof. K.P. Maity**, former Head of Mechanical Engineering Department, National Institute of Technology, Rourkela, for their kind support and concern regarding my academic requirements.

I am indebted to **Mr. Sushant Kumar Sahu, Mr. Debendra N Singh, Mr. Bikash Ranjan Moharana, Mr. Srikar Potnuru, Mr. Mantra Prasad Satpathy** and **Mr. Ranjan Hansda** for their support and co-operation which is difficult to express in words. The time spent with them will remain in my memory for years to come.

I thanks to Mr/s **Advanced Forming Technology Center (Regd.)** for their valuable cooperation during FEM analysis providing DEFORM[®]-3D software.

My parents deserve special mention for their inseparable support and prayers. They are the persons who show me the joy of intellectual pursuit ever since I was a child. I thank them for sincerely bringing up me with care and love.

Kanhu Charan Nayak

ABSTRACT

Combined extrusion-forging processes are now getting importance for its abilities to give improved material properties, high production rate and less material waste when compared with that produced by machining, casting or by assembling the individual parts produced by different manufacturing processes. In its simplest form of combined extrusion-forging process, a billet is forged by punch and dies with punch/die or both containing an opening for extrusion. This tooling arrangement permits the simultaneous lateral spread due to forging, and backward/forward extrusion or both forward and backward extrusion simultaneously through the die/punch opening(s). The flow pattern of the material is dependent on a number of factors, including the frictional conditions at the work piece/tooling interface; the geometry of the dies, particularly the size of the dies hole; the material type; and the percentage area reductions. Due to the complexity of the analysis, and because of the large number of process variables, it is difficult to estimate the forming force required to manufacture a given component. In this direction, the present work emphasizes on estimation of forming force for combined extrusion-forging process of regular shapes, micro hardness of component and study of grain structure. Experimental studies are carried out with a view to compare some of the simulation results predicted using finite element analysis, with that obtained from the experiment. Experiments are performed for male-female socket spanner or adopter using round aluminium billet and flat die in ambient temperature. Metal flow pattern and filling of die cavity are studied successfully from the experiment. FEM based commercial package DEFORM[®]-3D code is used for finite element analysis of the processes. Finite element analysis are carried out for the following characteristics; load versus punch displacement, effective stress, effective strain, total velocity and metal flow pattern. The results obtained from experimental investigation are found to be in good agreement with simulation results predicted by finite element analysis.

Keywords: Extrusion, Forging, Metal flow pattern, Finite element, Micro hardness, Flow stress, Friction factor

Contents

		Page No.
	ACKNOWLEDGEMENT	i
	Abstract	ii
	List of Tables	v
	List of Figures	vi
	NOMENCLATURE	ix
	CHAPTER 1 Introduction	1-7
1.1	Introduction	1
1.2	Research objective	6
1.3	Thesis outline	7
	CHAPTER 2 Literature review	8-11
2.1	Introduction	8
2.2	Study of previous work	8
2.3	Closure	11
	CHAPTER 3 Finite Element Analysis	12-27
3.1	Introduction	12
3.2	Pre-processor	14
3.2.1	Simulation control	14
3.2.2	Materials	14
3.2.3	Object description	15
3.2.4	Inter object relation	15
3.2.5	Movement control	15
3.2.6	Boundary condition	16
3.3	Simulation	16
3.4	Post-processor	16
3.5	Finite element based analysis of combined extrusion- forging process	17
3.6	Result analysis	20
3.6.1	Stress-strain and velocity of flow analysis	21
3.6.1.1	Socket/spanner adopter made by square punch and hexagon die	21
3.6.1.2	Socket/spanner adopter made by hexagon punch and hexagon die	22
3.6.1.3	Socket/spanner adopter made by square punch and square die	22
3.6.1.4	Socket/spanner adopter made by hexagon punch and	

	square die	23
3.6.2	Variation of punch load with punch displacement	24
3.7	Conclusions	26
CHAPTER 4	Experimental Analysis	28-53
4.1	Introduction to experimental analysis	28
4.2	The test rig	28
4.3	Experimental set up and procedure	40
4.4	Determination of stress-strain characteristic of aluminium	42
4.5	Determination of friction factor	44
4.6	Result analysis	46
4.6.1	Variation of punch load with punch displacement	46
4.6.2	Micro hardness and distortion of grain boundary	49
4.5	Conclusions	53
CHAPTER 5	Comparison of Results and Discussion	54-62
5.1	Comparison of results	54
5.1.1	Peak load of combined extrusion-forging	54
5.1.2	Deformed shape	54
5.1.3	Metal flow pattern	57
5.1.4	Variation of socket depth and extruded length	58
5.2	Conclusions	62
CHAPTER 6	Conclusions and Scope for future work	63-64
6.1	Conclusions	63
6.2	Scope for future work	64
REFERENCES		65
COMMUNICATIONS		71

List of Tables

Table No.	Title of Table	Page No.
Table 3.1	Process parameters used in simulation	19
Table 4.1	List of components	29
Table 5.1	Comparison of peak loads of combined extrusion forging process of four different types of socket adopter	54

List of Figures

Figure No.	Figure Title	Page No.
Figure 1.1	Schematic diagram of forming sequences in cold forging (extrusion) of a gear blank	2
Figure 1.2	Various types of extrusion forging techniques	3
Figure 1.3	Closed forged (extrusion) solid parts	4
Figure 1.4	Closed forged (extrusion) tubular or cup shaped parts	4
Figure 1.5	A photographic view of combined open die extrusion forging product	4
Figure 1.6	A typical product of forward-backward-radial process	5
Figure 1.7	Combined extrusion-forging products	6
Figure 3.1	Major input parameters for FEM simulation for combined extrusion forging process	12
Figure 3.2	Three major component of FEA	13
Figure 3.3	(a) Square-hexagon socket adopter, (b) Hexagon-hexagon socket adopter, (c) Square-square socket adopter and (d) Hexagon-square socket adopter.....	18
Figure 3.4	Sectional views with dimension of hexagon-hexagon and square-square socket adopter	18
Figure 3.5	Details diagram of die-punch set up with billet	20
Figure 3.6	From left to right; full view and sectional view of simulation set up	20
Figure 3.7	Distribution of strain-effective	21
Figure 3.8	Distribution of stress-effective	21
Figure 3.9	Distribution of stress-mean	21
Figure 3.10	Distribution of flow of total velocity	21
Figure 3.11	Distribution of strain-effective	22
Figure 3.12	Distribution of stress-effective	22
Figure 3.13	Distribution of stress-mean	22
Figure 3.14	Distribution of flow of total velocity	22
Figure 3.15	Distribution of strain-effective	23
Figure 3.16	Distribution of stress-effective	23
Figure 3.17	Distribution of stress-mean	23
Figure 3.18	Distribution of flow of total velocity	23
Figure 3.19	Distribution of strain-effective	23
Figure 3.20	Distribution of stress-effective	23
Figure 3.21	Distribution of stress-mean	24
Figure 3.22	Distribution of flow of total velocity	24
Figure 3.23	Variation of load with stroke for square-hexagon socket adopter	24
Figure 3.24	Variation of load with stroke for hexagon-hexagon socket	

	adopter	25
Figure 3.25	Variation of load with stroke for square-square socket adopter	25
Figure 3.26	Variation of load with stroke for hexagon-square socket adopter	26
Figure 4.1	Extrusion-forging die set up assembly	30
Figure 4.2	Container	31
Figure 4.3	Cover plate for container	32
Figure 4.4	Sleeve	33
Figure 4.5	Extrusion forging die holder	34
Figure 4.6	Punch with punch plate	35
Figure 4.7	Punch rod 2	36
Figure 4.8	Square punch head	36
Figure 4.9	Hexagon punch head	37
Figure 4.10	Circular die	37
Figure 4.11	Circular split die	38
Figure 4.12	Square groove split die	38
Figure 4.13	Hexagonal groove split die	39
Figure 4.14	Base plate	40
Figure 4.15	Photographic view of experimental set up with main components	41
Figure 4.16	Compression test set up with aluminum specimen	43
Figure 4.17	Stress-strain curves for aluminum	43
Figure 4.18	Set up for Ring test	44
Figure 4.19	Theoretical calibration curve for standard ring (6:3:2)	45
Figure 4.20	Various stages of combined extrusion-forging process	46
Figure 4.21	Variation of load with stroke for square-hexagon socket adopter	47
Figure 4.22	Variation of load with stroke for hexagon-hexagon socket adopter	47
Figure 4.23	Variation of load with stroke for square-square socket adopter	48
Figure 4.24	Variation of load with stroke for hexagon-square socket adopter	48
Figure 4.25	Different zones for measurement of micro hardness	49
Figure 4.26	Distribution of micro hardness at zone I	50
Figure 4.27	Distribution of micro hardness at zone II	50
Figure 4.28	Distribution of micro hardness at zone III	50
Figure 4.29	Grain structure of aluminium during extrusion forging process	52
Figure 5.1	Extrusion-forging shapes for four types of socket adopter	55
Figure 5.2	Die filling at different punch movement for four types of socket adopter	56
Figure 5.3	Flash gutter arrangement	56
Figure 5.4	Sectional view of Socket adopter	57
Figure 5.5	Metal flow patterns at different punch movement	58

Figure 5.6	Full photographic views of patterns of metal deformation in extrusion-forging	58
Figure 5.7	Socket depths and extruded length	59
Figure 5.8	Variation of socket depth and extruded length for square-hexagon socket adopter	60
Figure 5.9	Variation of socket depth and extruded length for hexagon-hexagon socket adopter	60
Figure 5.10	Variation of socket depth and extruded length for square-square socket adopter	61
Figure 5.11	Variation of socket depth and extruded length for hexagon-square socket adopter	61

NOMENCLEATURE

Symbol	Description
σ	Flow stress. MPa
k	Strength Coefficient, MPa
n	Strain hardening exponent
ϵ	Strain effective

*Dedicated
to my
Grandfather
and
Grandmother*

CHAPTER 1

INTRODUCTION

1.1 Introduction

Forming or metal forming, is the metalworking process of manufacturing metal parts and objects through mechanical deformation; the work piece is reshaped without adding or removing material, and its mass remains unchanged. This process has abilities to give improved material properties, high production rate and less material waste when compared with that produced by machining, casting or by assembling the individual parts produced by different manufacturing processes. Metal forming includes (i) massive forming processes such as forging, extrusion, rolling and drawing and (ii) sheet forming processes such as deep drawing, brake forming and stretch forming. Massive forming processes, which includes forging and extrusion process is classified as follows:

- (a) Closed-die forging with flash and without flash, (b) Coining, (c) Electro upsetting, (d) Forward extrusion forging, (f) Back ward extrusion forging, (g) Hobbing, (h) Isothermal forging, (i) Nosing, (j) Open-die forging, (k) Orbital forging, (l) Radial forging and (m) Upsetting

Depending on the direction of the punch movement and the direction of the material flow, extrusion process is classified into three basic types, named as a forward (direct) extrusion, backward (indirect) extrusion and radial/lateral extrusion. In addition to the basic extrusion operation, there are some combined extrusion processes in which two (or more) basic extrusion processes and/or forging processes occur simultaneously.

Extrusion-forging is a bulk metal forming operation in which the cross-section area of the billet is reshaped and changed into a certain shape by forcing it through a narrow path called extrusion die and obtaining a desired shape at the end of the billet or at other locations by filling the forging die cavity. A variety of regular/irregular cross-sections and complex

shape can be achieved by this process. This process has a definite advantage over other production processes used to manufacture complicated sections having re-entrant corners. Large reduction achieved even at high strain rates has made this process is one of the fastest growing metals working methods.

In combined forward-backward extrusion forging process, the billet is reshaped and changed into certain shape (triangular, square, pentagon, hexagon, gear, box spanner, male female adopter) by forcing it through a narrow extrusion-forging die set up.

Cold extrusion is a special type of forging process wherein cold metal is forced to flow plastically under compressive force into a variety of shapes. The shapes are axisymmetric with relatively small non symmetrical features. Several forming steps are used to produce a final part of relatively complex geometry starting with billet of simple shape as shown in Figure 1.1 [1]. Some basic techniques of cold forging-extrusion are illustrated in Figure 1.2 [2]. Through combination of these techniques, a very large number of parts can be produced, as illustrate schematically Figure 1.3 and 1.4 [2].

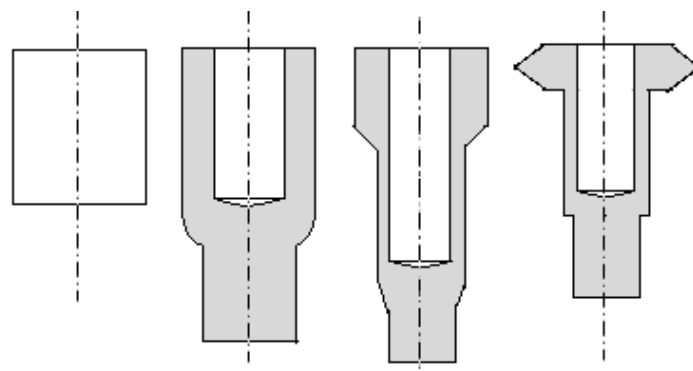
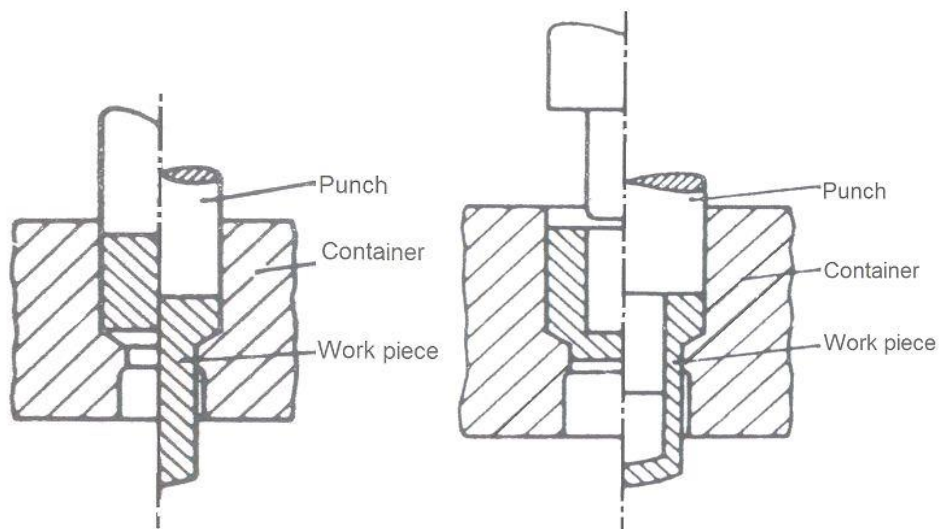


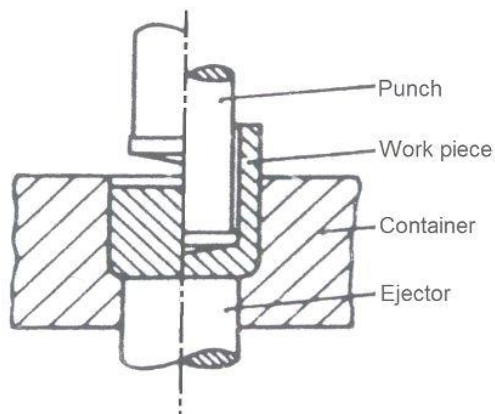
Figure 1.1 Schematic diagram of forming sequences in cold forging (extrusion) of a gear blank [1]

From above figure, left to right: blank, simultaneous forward rod and backward cup extrusion, back ward cup extrusion and simultaneously upsetting of flange and coining of shoulder.

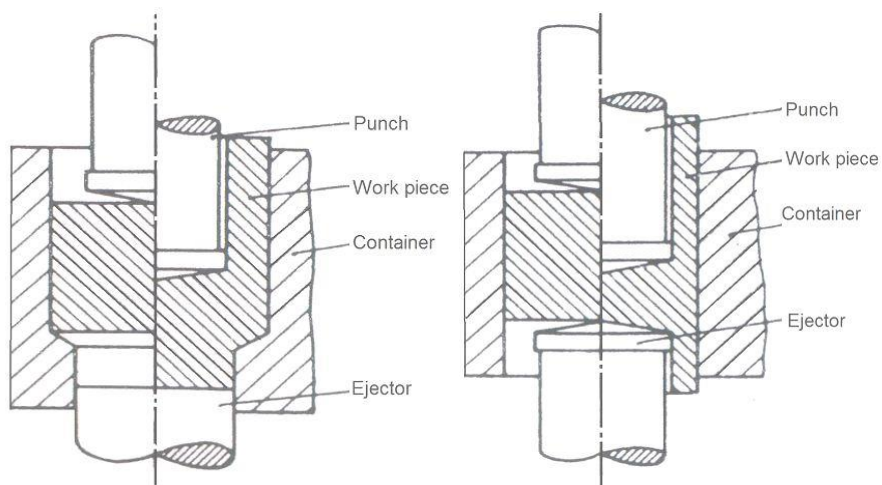


(a) Forward rod extrusion

(b) Forward cup extrusion



(c) Back ward cup extrusion



(d) Combined forward rod and backward cup extrusion

(e) Combined forward and backward cup extrusion

Figure 1.2 Various types of extrusion forging techniques [2]

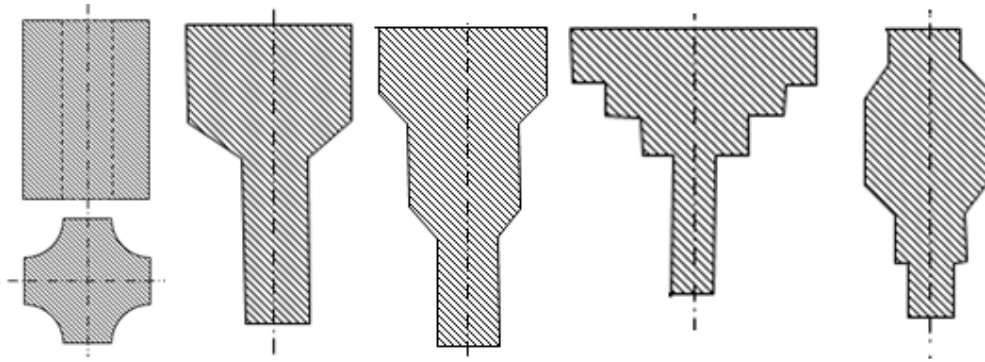


Figure 1.3 Closed forged (extrusion) solid parts [2]

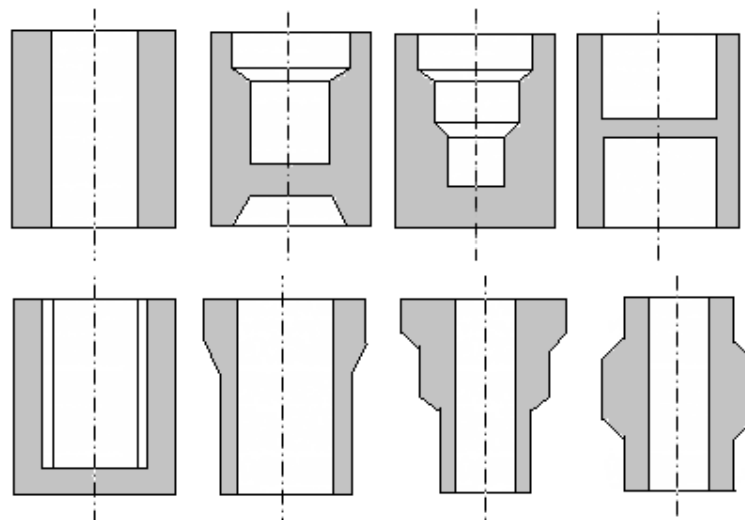


Figure 1.4 Closed forged (extrusion) tubular or cup shaped parts [2]

Near net shape of many components with different materials are produced by extrusion forging processes and forward backward radial extrusion as illustrate in Figure 1.5 and 1.6 [3, 4].



Figure 1.5 A photographic view of combined open die extrusion forging product [3]



Figure 1.6 A typical product of forward-backward-radial process [4]

The variables influencing an extrusion-forging process are: (i) percentage of area reduction, (ii) dies geometry, (iii) product geometry, (iv) speed of extrusion, (v) billet temperature, and (vi) lubrication between the die and extruding material. In an industrial application, the above parameters should be suitably optimized to achieve the best results. The ram speed and temperature have a major influence on plastic properties of the billet material, and their effect can be studied by choosing a suitable constitutive equation.

Applications: Combined extrusion-forging process is used for the production of components of various shapes for different industries including automotive, air craft, agricultural implements, electrical, construction equipment, defence, etc. Other applications are; Stepped or tapered-diameter solid shafts, tubular parts with multiple diameters cylindrical, conical or other non-round holes, hollow parts having a closed end, cupped parts with holes that are cylindrical, conical shapes, net- and near-net shape forgings for aircraft industry, nuts and bolts, flanged shafts, box spanner, male female adopter. Some of the applications are shown in Figure 1.7.





Figure 1.7 Combined extrusion-forging products

1.2 Research Objective

The present work emphasizes on estimation of forming force for combined extrusion-forging process of regular shapes, micro hardness of component and study of grain structure. Experimental studies are carried out with a view to compare some of the simulation results predicted using finite element analysis (FEA), with that obtained from the experiment. Experiments are performed for different types of male-female socket spanner or adopter. A combined extrusion forging test rig is designed and developed for the said purpose and all

experiments are carried out using round shape aluminium billet. Finite element method based commercial package DEFORM[®]-3D code is used for FEA of the processes for simulation analysis. Implementing finite element analysis following characteristics is studied; load versus punch displacement, effective stress, effective strain, total velocity and metal flow pattern. The results obtained from experimental investigation are compared with simulation results predicted by finite element analysis.

1.3 Thesis outline

Chapter 2: Literature review

Includes a literature study to contribute the basic knowledge which already available involving the types and significant of metal forming analysis and types of combined extrusion forging.

Chapter 3: Finite element analysis

This chapter deals with finite element analysis of combined extrusion forging process for different types of socket adopter.

Chapter 4: Experimental analysis

This chapter gives a description about experimental set up and design to produced four different types of socket adopter. Also deals with determination of characteristics of aluminium material.

Chapter 5: Comparison of results and discussion

Includes analysis of results obtained from finite element analysis and from experiment.

Chapter 6: Conclusions and scope for future work

This chapter deals with the conclusions and scope for future work.

CHAPTER 2

*LITERATURE
REVIEW*

2.1 Introduction

One of the current challenges faced by the manufacturing industry is to produce component of high strength, resistance to fatigue, heat, corrosion and low production cost. Forming is one such process, which has the additional advantage of greater utilization of raw materials and high productivity apart from above advantage. Among all forming processes combined extrusion-forging is a process where difficult to produce shapes, can be formed with higher mechanical properties and near net shape production can be achieved.

2.2 Study of Previous work

Vickery and Monaghan [5] present results obtained from an experimental and analytical investigation of a combined forging-extrusion process applied to an axisymmetric component. They established that the forging-extrusion process consisted of three distinct stages. Narayanasamy et al. [6] has carried out an experimental investigation of aluminium alloy billets during extrusion-forging using different lubricants. It is observed that the protrusion height increases with the increase in the approaching angle for a given extrusion load. The relationship among the various bulge parameters namely the hoop stress, the hydrostatic stress and the stress ratio parameters are also established. The flow pattern of the material is dependent on a number of factors, including the frictional conditions at the work piece/tooling interface and the geometry of the dies [7]. MacCormack and Monaghan analysed [8] the combination of extrusion and forging of very complex shape of spline geometry. Forming pressure depends on the ram speed. The forming load increased with increase in ram speed (0.4-0.6mm/sec) [9]. Material flow of aluminium alloy was studied by Uyyuru et al. [10] in backward cup extrusion. Ketabchi et al. [11] investigated the effect of punch speed and work piece temperature on backward extrusion. They studied simulation

result for effective stress, effective strain and prediction of good accuracy of backward extrusion load.

Zaeem et al. [12] carried out cyclic forward-backward extrusion of aluminum rods for producing ultrafine grained. They concluded that , due to CFBE grain size reduces, yield strength and tensile strength increases 3.5 and 3 times greater than that the initial. Sadough et al. [13] investigates the rheological behaviour microstructure and hardness of aluminum alloy using backward extrusion. They summarised that, the hardness increases with decrease in temperature and wall thickness. During the forging-extrusion process, several barrels with radius of different curvature successively formed along the lateral free surface of the work piece. Due to this formation, fold defects are developed around the equatorial plane of the workpiece under various combinations of process parameters [14].

Moshksar and Ebrahimi [15] carried out the backward extrusion forging of a regular polygon cup shaped components. They find that, velocity field approach can be used correctly for prediction of extrusion load and configuration of nosed punch in backward extrusion forging. Giardini et al. [16] presented the influence of die geometries and lubrication conditions in extrusion-forging process (closed die forging). They focused on ductile fracture phenomenon and material flow, taking these two conditions as formability index. An analytical approach to examine the deformation was presented by Brayden and Monaghan [17] during an extrusion/forging operation. They developed velocity fields which were obtained from a number of experimental tests. These velocity fields are used in upper bound technique to evaluate the load and stress during an extrusion-forging process. Lee et al. [18] used upper bound element technique to investigate the forward and backward extrusion of hexagonal- and trochoidal shaped wrench bolts. Yamin et al. [19] studied the impact of deformation, temperature and the lubrication to the plastic properties of magnesium alloy by conducting a series of experiments of cup-rod combined extrusion processes.

Wang et al. [20] modify the manufacturing of the support shaft in the automobile industry to minimizing the waste material and improving the properties of shaft by implementing extrusion-forging process. It includes two stage extrusion processes and whole process is simulated and verified by finite element method. Patra and Sahoo [21] proposed theoretical analysis based on upper bound technique and experimental investigation for extrusion-forging of the pentagonal head with round shaft from cylindrical billet through square flat die. Patra et al. [22] carried out the experimental studies with a view to comparing some of the theoretical results predicted (using SERR analysis) with that obtained from the experiment and explore the metal flow pattern. Qamar [23] investigates the effect of shape complexity on the dead metal zone (DMZ) and metal flow through cold extrusion experiments and finite element simulations on some solid profiles. He performed the experiments using flat-face dies of different complexities and different billet materials. 2D and 3D finite element simulations were carried out. Kim et al. [24] developed the finite volume method for investigating the effects of solid lubricants in aluminium backward extrusion processes. Various shear friction factors are used for this numerical study. Lubrication is found to have a significant effect on the final shape in backward extrusion. In most of the forging cases, upper bound element technique is used for axisymmetric forging parts by forward and backward simulation [25, 26]. Cho et al. [27] carried out numerical simulation of the cold forging operation on the basis of theoretical knowledge on process design using the finite element software. The deformation behaviour, the metal flow modes, the forming load, the deformation energy, and the filling of the die cavity were the features of interest in many researches. For example, Hashmi and Klemz [28] used a theoretical analysis to predict the deformation profile of a cylindrical billet and effect of material properties, product design in the extrusion-forging process. Hu and Hashmi [29] studied the variations of billet profile and of the needed load during the extrusion forging stage of a

rectangular billet of lead using the finite element method and experimentally. This finite element method was also used to study the influence of die geometry, die shapes with different draft angles, fillet radii and frictional condition in the combined extrusion-forging operation on the ductile fracture criterion and flow of material [30-32]. A series of experiment were conducted by Chitkara and Bhutta [33] for incremental near-net shape heading of a circular rod to form a round but tapered bolt with a flat square head at one end. And the process is simulated using free body equilibrium approach based on the slab method of analysis and an upper bound analysis. They also conducted the experiment and did the theoretical analysis for incremental forging and heading of solid and hollow splines/spur gear [34, 35]. Many researchers are analysed the control of material flow and limits of lubrication in forward backward extrusion by FEA and experimentally [36, 37]. Many researchers are used Deform 3D as an important physical modelling tool for investigation of metal flow, die fill, effective/mean stress, effective strain, strain rate etc, which are influence by various factors like machining parameter (ram speed), friction at die/punch-work piece interface, shape of the product geometry, die geometry, properties of work material and type of metal working process such as extrusion, forging, combined extrusion forging (both for cold and hot working) the simulation of combined extrusion forging process for different shapes [38-42].

2.3 Closure

From the reviewed papers, it is observed that, lot of works are carried out and analysed on extrusion-forging for the different sections from cylindrical billet. Till now, many complicated different shapes which are manufactured by machining process can be produced by combined extrusion-forging are not analysed. The present work attempts to fill this gap and gives a sincere effort to extend the combined extrusion-forging of different socket adopters. The results are also validated with that of experimental and finite element analysis.

CHAPTER 3

*FINITE ELEMENT
ANALYSIS*

3.1 Introduction

Metal forming is especially attractive in cases where the part geometry is moderate complexity and the production volume are large, so that tooling costs per unit product can be kept low. It is accomplished by extensive previous experience and an expensive and time consuming cycle of trials, evaluations, redesign, analysis and optimization of process. Design approach for such metal forming process in manufacturing is rapidly being replaced by more efficient computer simulation. In recent decay, computer modeling is routinely used by industry for fast evaluation and optimization of forming processes before any actual physical trial. In our present analysis DEFORM[®]3D is used to simulate the forming (combined extrusion and forging) process to get the proposed product shape. Major input requisite for simulation is listed below Figure 3.1

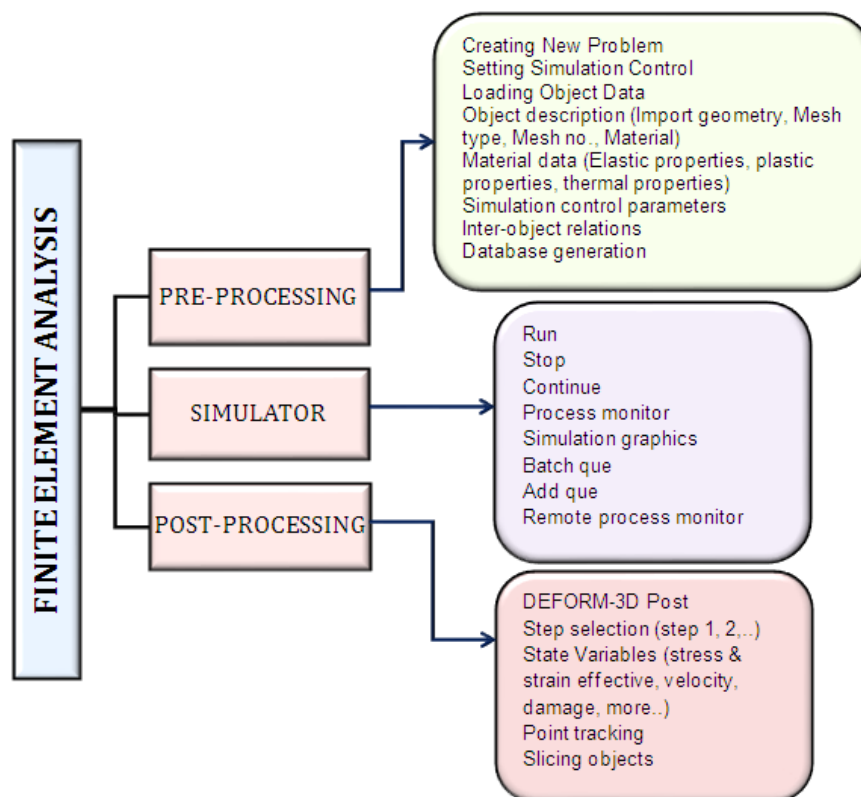


Figure 3.1 Major input parameters for FEM simulation for combined extrusion forging process

Total system consists of three major components

- (i) Pre-processor: Design to establish the input conditions of the forming process analysis.
- (ii) Simulation: According to input data the finite element simulation performs the numerical calculations to solve the problem.
- (iii) Post-processor: A post-processor for reading the database files from the simulation engine and displaying the results graphically and for extracting numerical data. The postprocessor is used to view simulation data after the simulation has been run. The postprocessor features a graphical user interface to view geometry, field data such as strain, temperature, and stress, and other simulation data such as die loads. The postprocessor can also be used to extract graphic or numerical data for use in other applications. All three processes with output are shown in Figure 3.2.

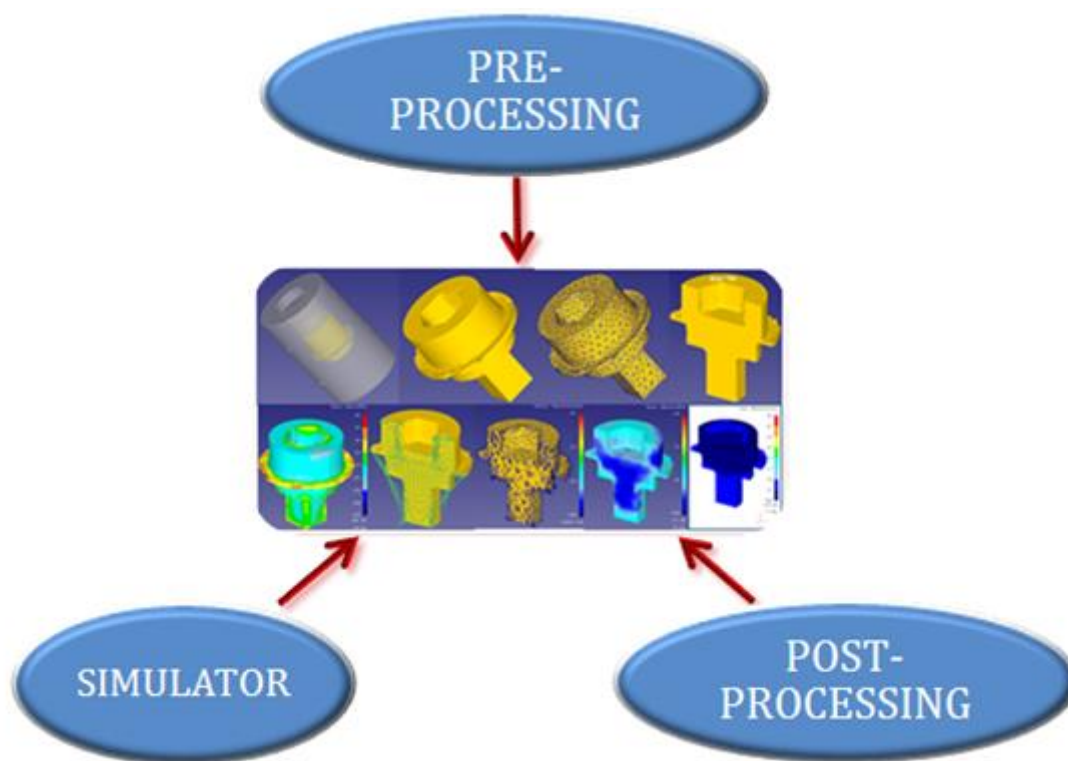


Figure 3.2 Three major component of FEA

3.2 Pre-Processor

3.2.1 Simulation control

Herein simulation SI unit convention, implicit langrangian incremental type formulation and deformation mode of simulation are followed. The finite element mesh is generated to the work piece and follows its deformation. The primary die is the punch or ram for which stopping and stepping criteria are defined. Stopping is terminating the simulation when the distance between reference points on two objects/dies reaches the specified distance. Stopping distance are in conjunction with the reference points. Solution step size or stepping criteria can be controlled by time step or by displacement of the primary die. If the stroke per step is specified, the primary die will move the specified amount in each time step. The total movement of the primary die will be the speed assigned to the punch multiplied by the total number of steps. For present simulation die displacement method of stepping criteria is defined. Remeshing is the process of replacing a distorted mesh with a new undistorted mesh and mesh. The iteration controls specify criteria the FEM solver uses to find a solution at each step of the problem simulation. Conjugate-Gradient solver and direct iteration are opted. Convergence problems are well suited for Conjugate-Gradient. Appropriate constant values are automatically set SI units.

3.2.2 Materials

The material model used in this study was isotropic and rigid-perfectly plastic. The material chosen is commercially available aluminum. Stress required for deformation (flow stress) is generally given as power equation which is a function of strain-hardening exponent and strength coefficient. The flow stress governing equation is followed by the equation (4.1). The numerical value of flow stress is 282 MPa (from experiment).

3.2.3 Object description

In this simulation shaped forging die and different shape of punch are taken. Square and hexagonal headed punch shapes are considered as primary die or top die. These are considered as rigid objects and made of non-deformable materials. The rigid objects are modeled in solid modeling software and STL files are imported for simulation during defining the geometry. The plastic object is the billet/work piece and cylindrical in shape. The geometry of the billet is also generated by using solid modeling software. Tetrahedral shape, 15000 numbers of initial elements and finer internal mesh were generated for billet. Ambient temperature is considered for the simulation.

3.2.4 Inter-object relation

The purpose of inter-object relations is to define how the different objects in a simulation interact with each other. All objects which may come in contact with each other through the course of the simulation must have a contact relation defined. In this simulation, a deforming work piece is being deformed between two rigid dies. The rigid die or top die defined as the master die and the billet is defined as slave object. It is very important to define these relationships correctly for a simulation to model a forming process accurately. The critical variables to be defined between contacting objects are:

- ❖ Friction factor: 0.156 (from ring test, described in section 4.5).
- ❖ Interface heat transfer coefficient: The interface heat transfer coefficient specifies the coefficient of heat transfer between two objects in contact. If no data is available, value 0.004(English) or 11 (SI, system defined default value) is considered for heat transfer coefficient which gives reasonable results.

3.2.5 Movement control

Movement controls can be applied to rigid objects and boundary nodes of meshed objects. Speed with –z direction movement of ram at a speed of 1mm/min was opted. Total

forging stroke is chosen according to the setting of die and filling of metal in die cavity which is equal to the top die displacement.

3.2.6 Boundary condition

The top die or punch movement is only in $-z$ direction. There was no movement of bottom die and billet.

3.3 Simulation

When all requisite data are given in the pre-processor steps the simulation system checks for any missing data and generates a database. The simulation starts and initiates a series of operations to run the simulation and generate new meshes as necessary. Run-time information will be written to the ProblemId.MSG and ProblemId.LOG files. Execution information, including convergence information for each step and simulation error messages, can be found in the .MSG file. Information on simulation and remeshing, execution times, and fatal errors can be found in the .LOG file or in the command window where DEFORM was executed from.

3.4 Post-Processor

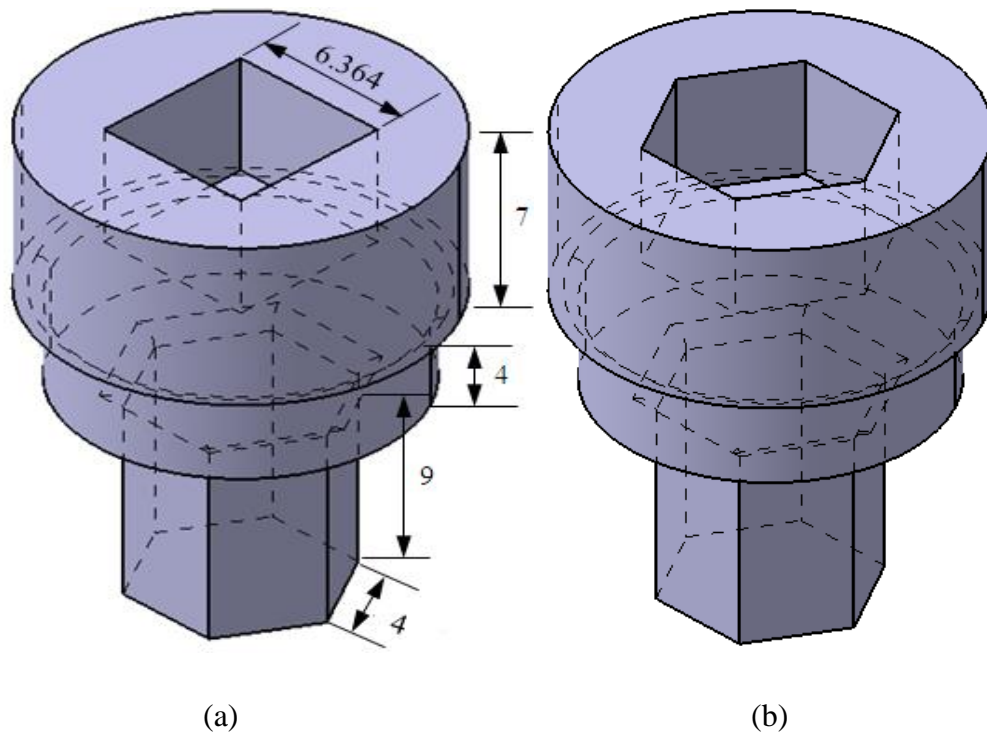
Post processor with a variety of features and graphics allows engineers to check the model results and present them in a way to understand the model results in an efficient manner. The post-processor is used to view and extract data from the simulation results in the database file. All results steps which were saved by the simulation engine are available in the post-processor. Information which is available from the post-processor includes:

- ❖ Deformed geometry, including tool movements and deformed mesh at each saved step.
- ❖ Contour plots: Line or shaded contours display the distribution of any state variables, including stress, strain, temperature, damage, and others.
- ❖ Vector plots: displacement and velocity vectors indicate magnitude and direction of displacement or velocity for every node at each step throughout the process.

- ❖ Graphs of key variables such as press loads, volumes, and point tracked state variables.
- ❖ Point tracking to show how material moves and plots of state variables at these points.
- ❖ Flow net showing material flow patterns on a uniform grid. Generally a very good predictor of grain flow patterns in the finished part.
- ❖ State variables can be tracked between any two points and plotted in a graph format. The state variables can either follow the boundary or linearly between the points.
- ❖ A histogram plot of any state variable can be made to view the distribution of any given state variable throughout a body.

3.5 Finite element based analysis of present problem

Commercially available FE-based Deform 3D software is used for the simulation of four different types of male female socket spanner/adaptor of aluminium rod. Brief descriptions about details drawing of socket adaptors are shown in Figure 3.3. Sectional view of hexagon-hexagon socket adaptor and square-square socket adaptor with dimension is shown in Figure 3.4.



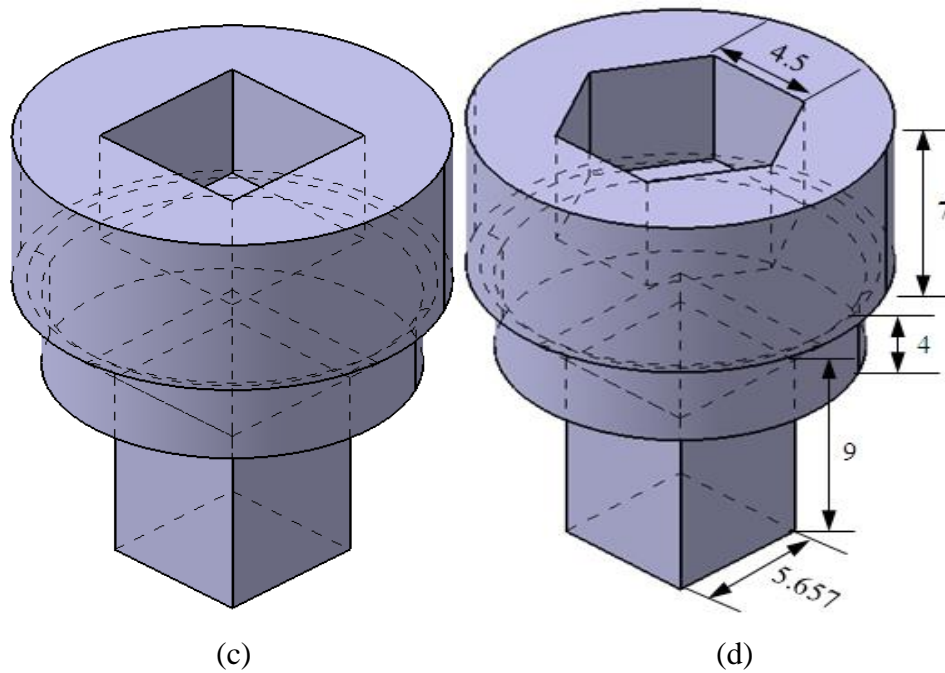


Figure 3.3 (a) Square-hexagon socket adapter, (b) Hexagon-hexagon socket adapter, (c) Square-square socket adapter and (d) Hexagon-square socket adapter

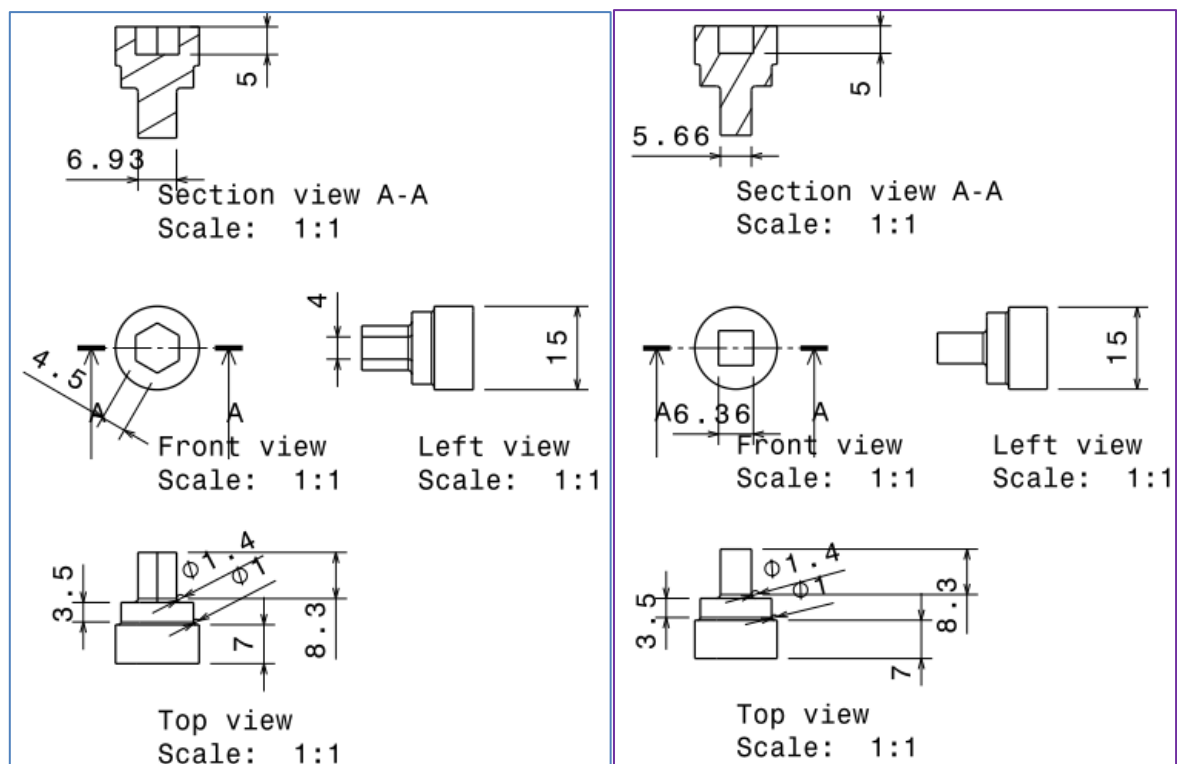


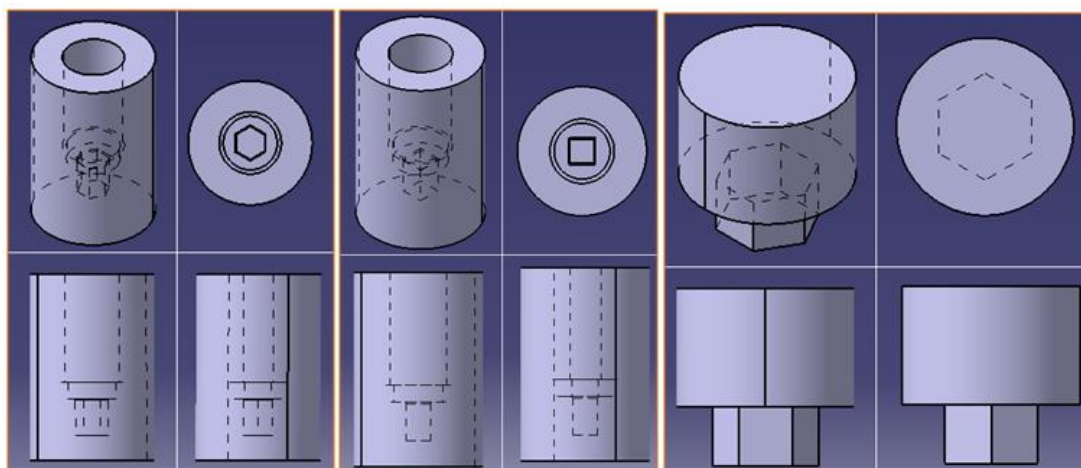
Figure 3.4 Sectional views with dimension of hexagon-hexagon and square-square socket adapter

Above drawing gives details dimension of all four different types of socket adopter. The process parameters used in this simulation are summarized in Table 3.1. These tabulated data and the dimensions are used for simulation process.

Table 3.1: Process parameters used in simulation

Billet length	13mm
Billet diameter	15 mm
Billet temperature	Ambient
Punch speed	1 mm/sec
Friction factor	0.156
Flow stress	282 MPa
No. of mesh element	15000
Average strain rate	1/sec
Limiting strain rate	0.01/sec

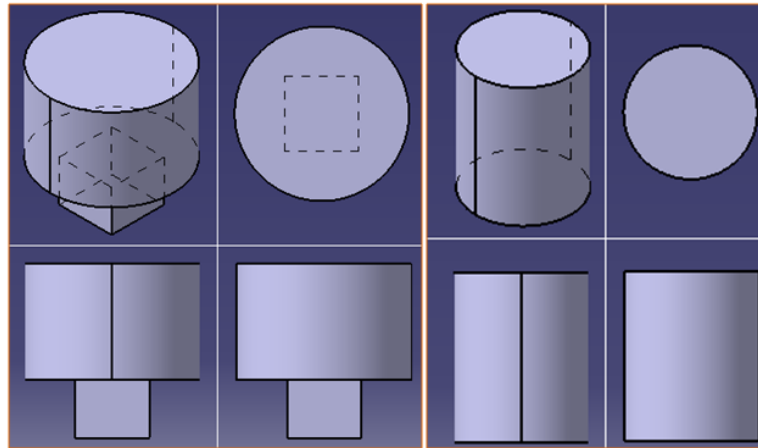
Figure 3.5 illustrate the details schematic diagram of die-punch set up modelled by CATIA, which are used in simulation for FEA after converting to .stl file. Sectional view of arrangement of die, punch and billet for the simulation is shown in Figure 3.6. In this figure a particular socket spanner/adopter is shown after deformation. Bottom die and container is combined and form a single object. Three objects (punch or top die, bottom die with container and billet) are imported to simulation for analysis of various characteristics.



(a) Hexagon die

(b) Square die

(c) Hexagon punch



(d) Square punch

(e) Billet

Figure 3.5 Details diagram of die-punch set up with billet

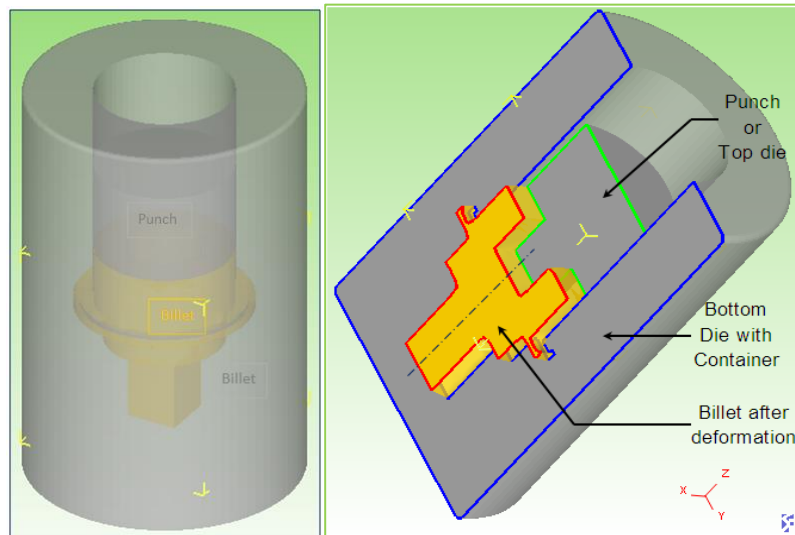


Figure 3.6 From left to right; full view and sectional view of simulation set up

3.6 Result analysis

Result obtained from the simulation process of combined extrusion-forging of four type of socket adopter are discussed and summarised. Here for the present analysis following simulation results are obtained; stress-strain analysis, total velocity of flow and variation of punch load with punch displacement.

3.6.1 Stress-strain and velocity of flow analysis

FEA are carried out for all types of socket adopter. In this analysis following characteristics are analysed; strain-effective, stress-effective, stress-mean and total velocity of flow. These are discussed separately for all socket adopter.

3.6.1.1 Socket spanner/adopter made by square punch and hexagon die

The simulated shape is analysed and different characteristics like strain effective, stress effective, stress mean and total velocity are discussed. The distribution of above said characteristics through out of the component are shown in Figure 3.7-3.10.

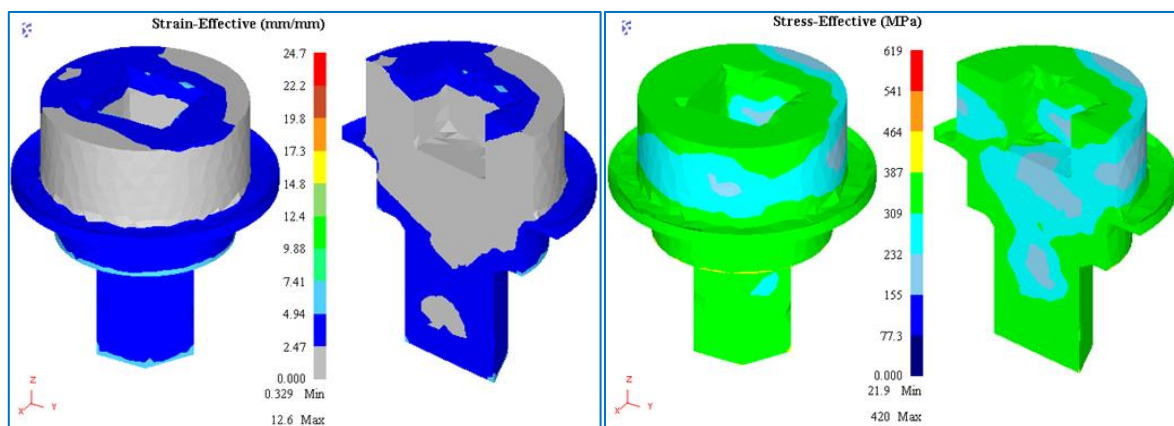


Figure 3.7 Distribution of strain-effective

Figure 3.8 Distribution of stress-effective

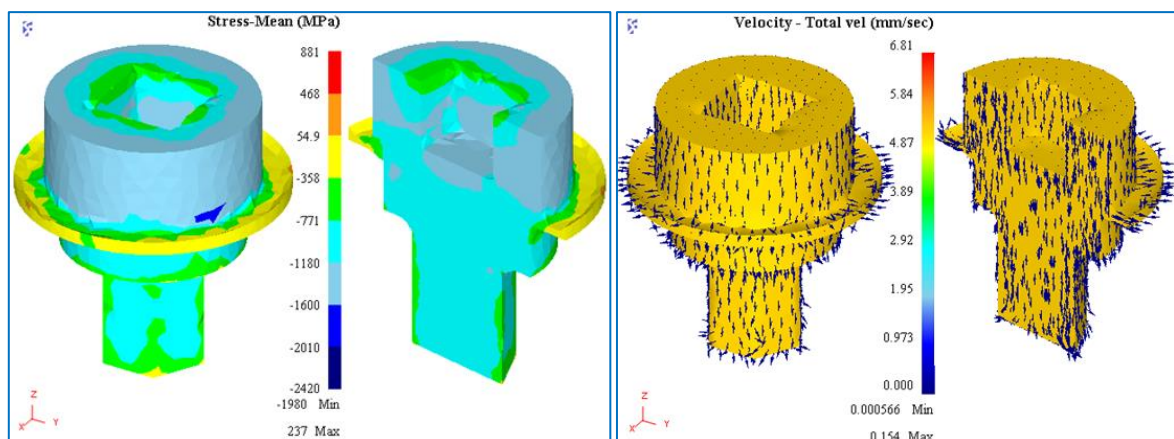


Figure 3.9 Distribution of stress-mean

Figure 3.10 Distribution of flow of total velocity

3.6.1.2 Socket spanner/adopter made by hexagon punch and hexagon die

The simulated shape is analysed and different characteristics like strain effective, stress effective, stress mean and total velocity are discussed. The distribution of above said characteristics through out of the component are shown in Figure 3.11-3.14.

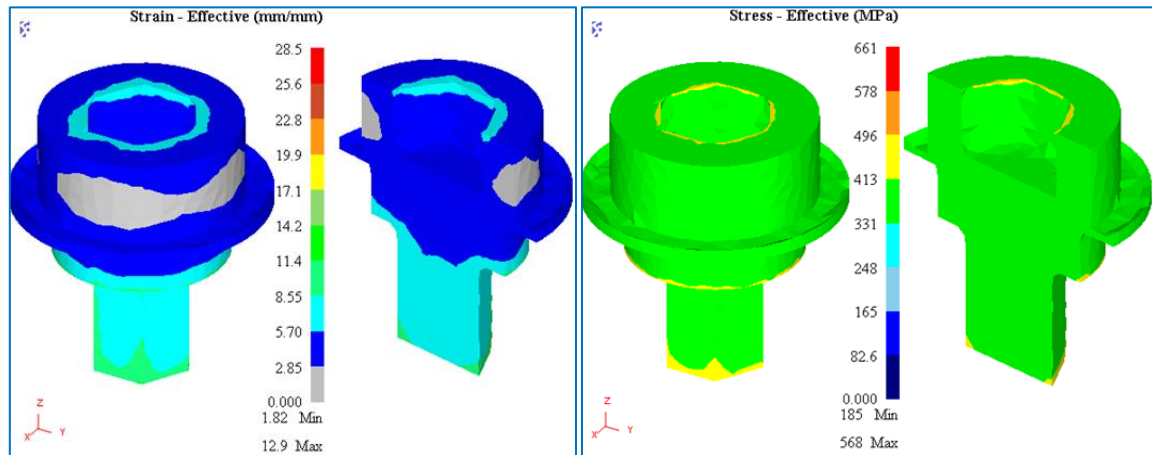


Figure 3.11 Distribution of strain-effective

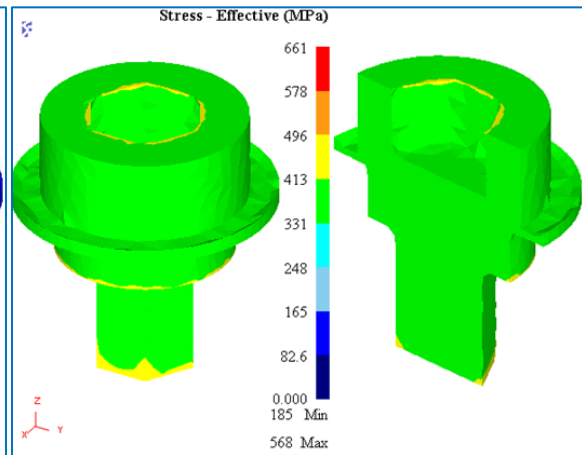


Figure 3.12 Distribution of stress-effective

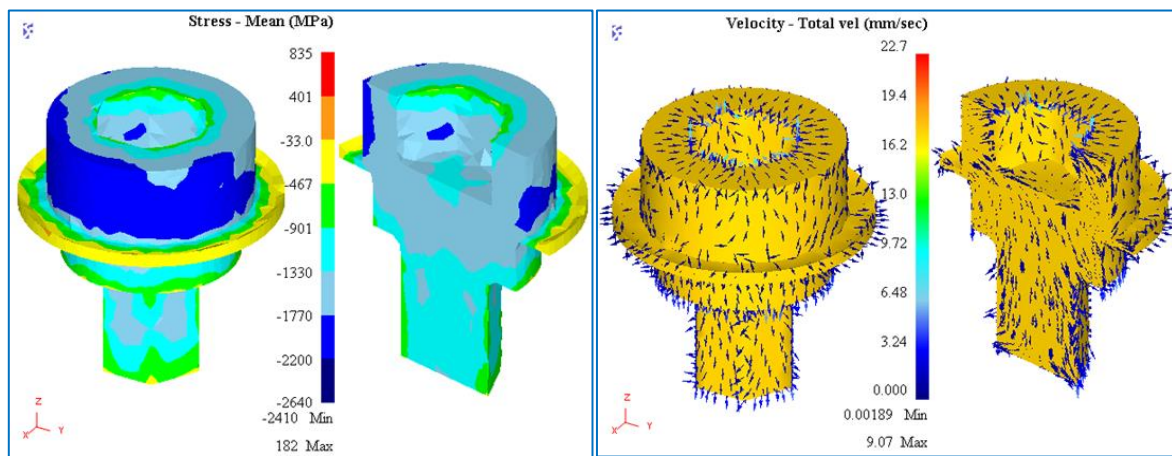


Figure 3.13 Distribution of stress-mean

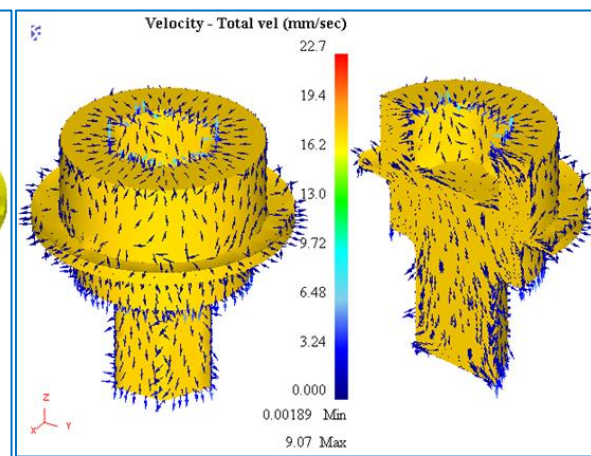


Figure 3.14 Distribution of flow of total velocity

3.6.1.3 Socket spanner/adopter made by square punch and square die

The simulated shape is analysed and different characteristics like strain effective, stress effective, stress mean and total velocity are discussed. The distribution of above said characteristics through out of the component are shown in Figure 3.15-3.18.

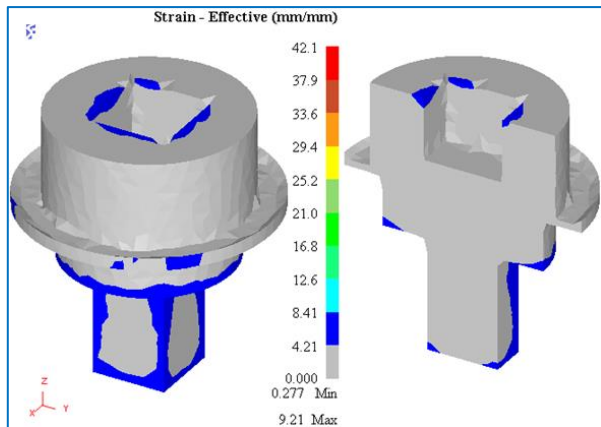


Figure 3.15 Distribution of strain-effective

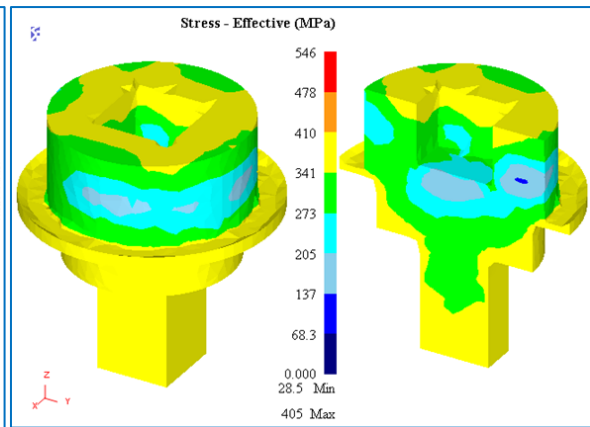


Figure 3.16 Distribution of stress-effective

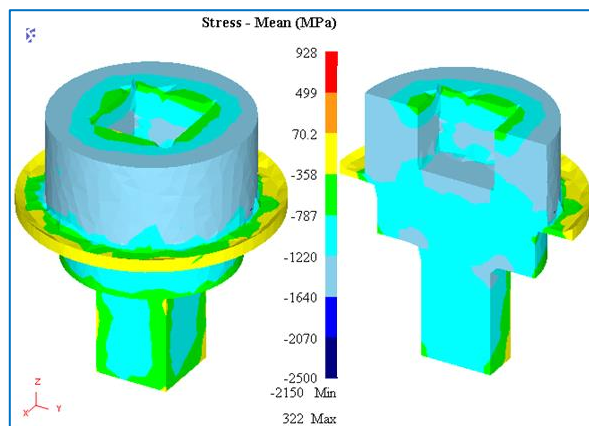


Figure 3.17 Distribution of stress-mean

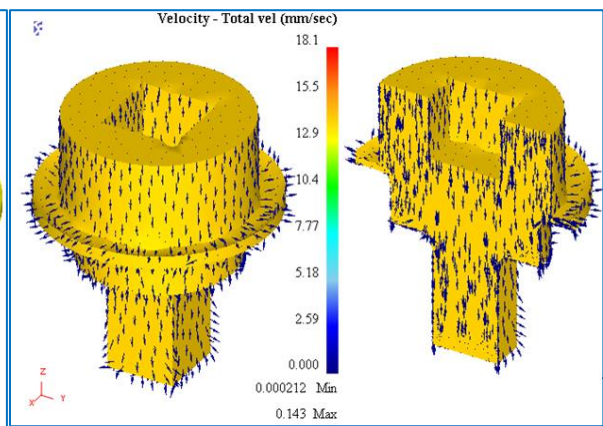


Figure 3.18 Distribution of flow of total velocity

3.6.1.4 Socket spanner/adopter made by hexagon punch and square die

The simulated shape is analysed and different characteristics like strain effective, stress effective, stress mean and total velocity are discussed. The distribution of above said characteristics through out of the component are shown in Figure 3.19-3.22.

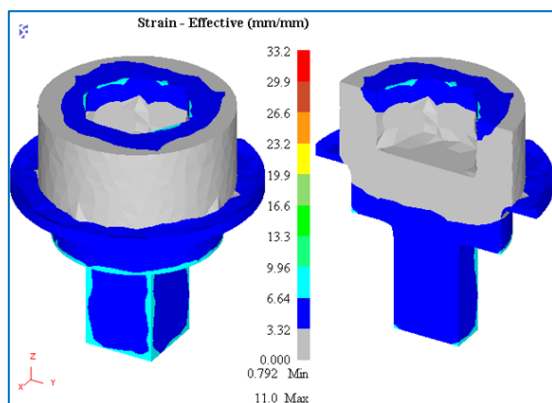


Figure 3.19 Distribution of strain-effective

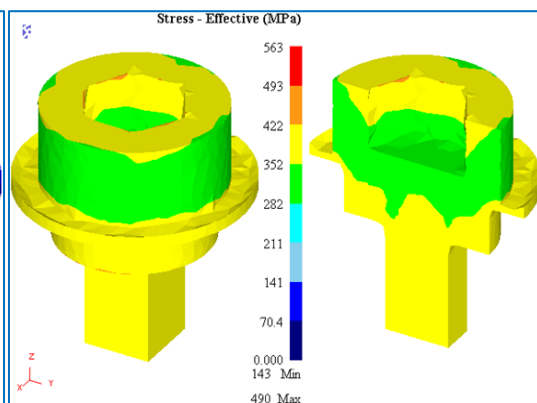


Figure 3.20 Distribution of stress-effective

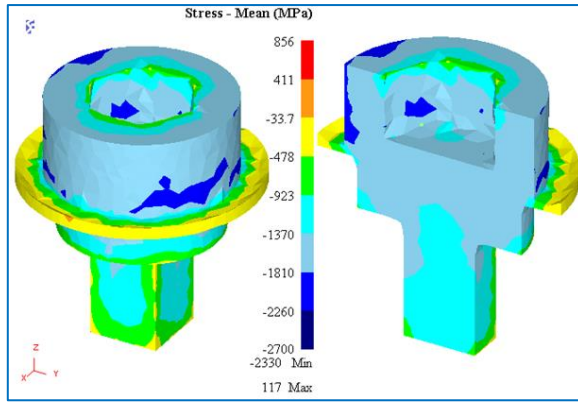


Figure 3.21 Distribution of stress-mean

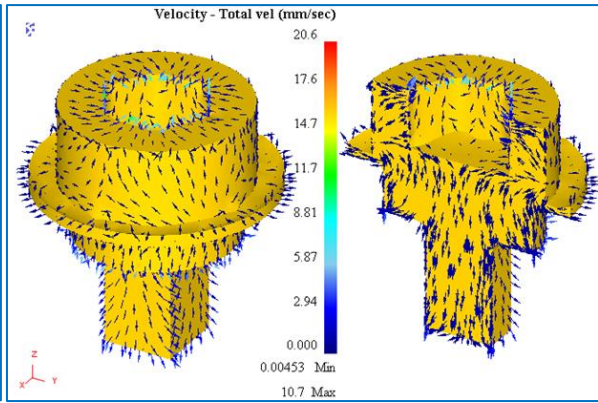


Figure 3.22 Distribution of flow of total velocity

3.6.2 Variation of load with punch displacement

The dies and punch plate used for simulation was same as that of experimental sets. Figure 3.23-3.26 gives variation of punch load with punch movement for different socket spanner/adopter. At the end of simulation the punch take high load because of final forging process take place before the extrusion and filling of edge and corners of die cavity.

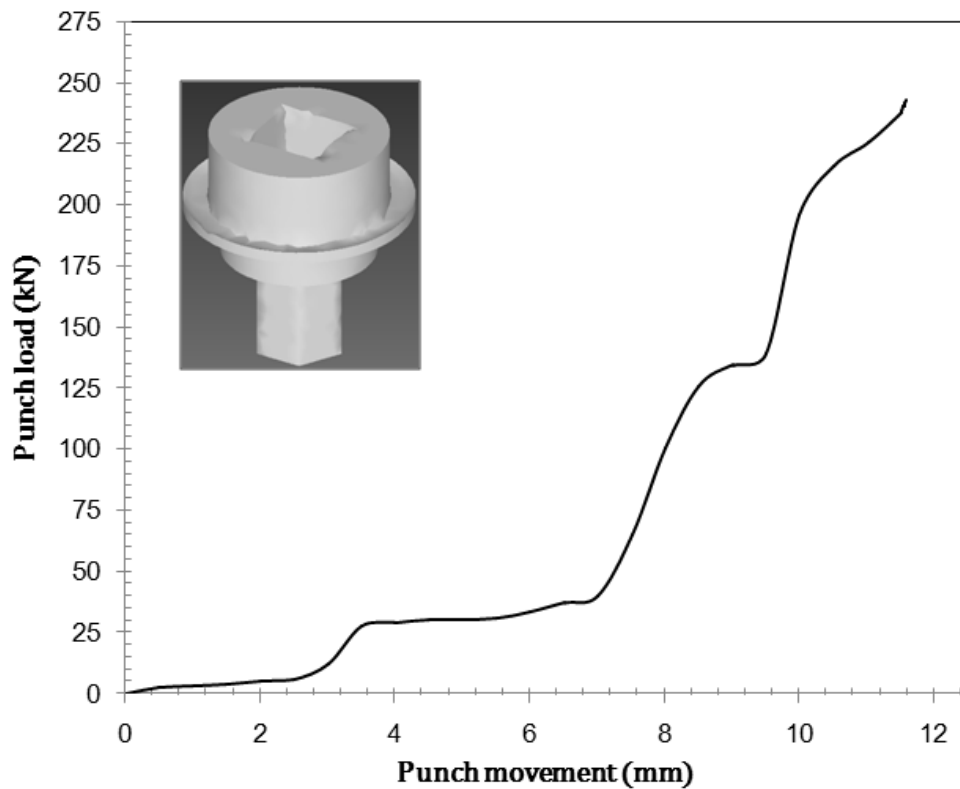


Figure 3.23 Variation of load with stroke for square-hexagon socket adopter

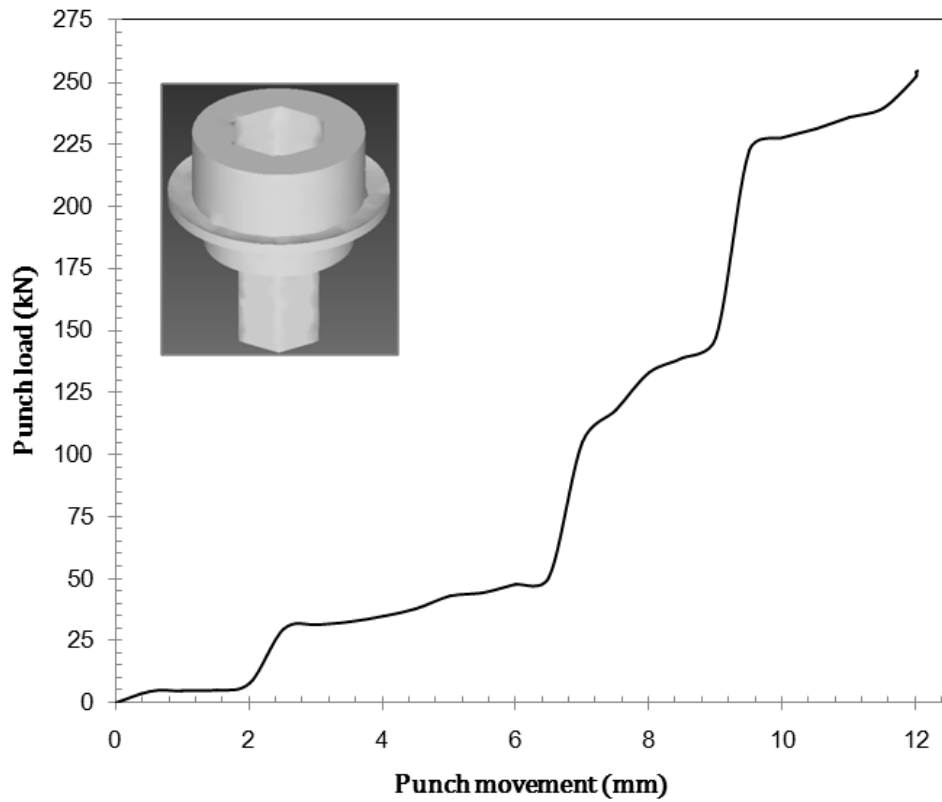


Figure 3.24 Variation of load with stroke for hexagon-hexagon socket adopter

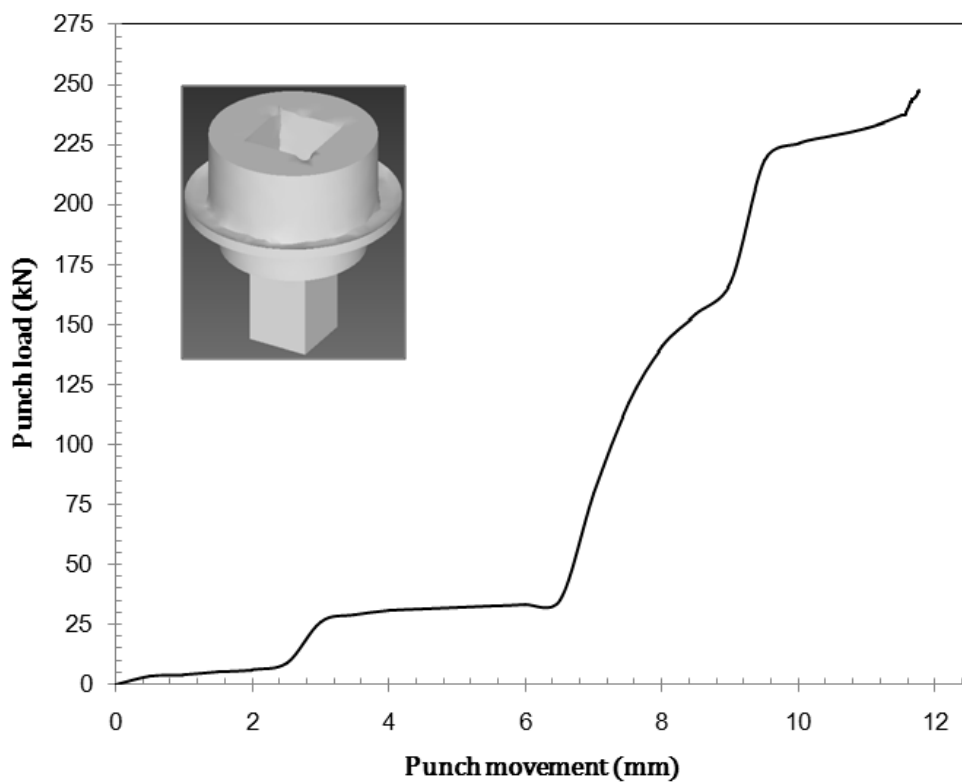


Figure 3.25 Variation of load with stroke for square-square socket adopter

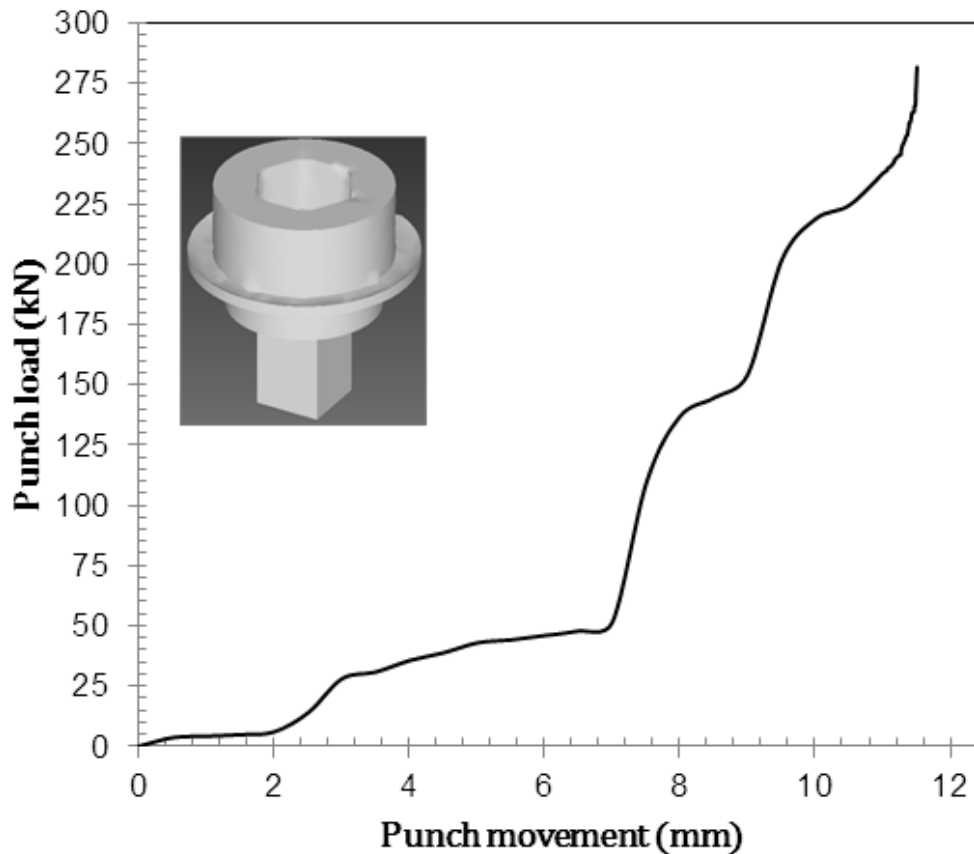


Figure 2.26 Variation of load with stroke for hexagon-square socket adapter

Initial compression of the billet occurs inside the extrusion-forging die with a punch displacement of approximately 2.4 mm for square-hexagon socket adapter (Figure 5.17) and square-square socket adapter (Figure 5.19). This shows that when the shape punch (square) is same, equal punch displacement is required for initial compression. Similarly approximately 2 mm punch movement is required for initial compression of other two socket adapter. This indicates that for the socket adapter, punch movement of initial compression depends upon the shape of the punch head (here square head or hexagon head punch).

3.7. Conclusions

Finite element analysis is implemented successfully for analysis of combined extrusion forging process. It gives the visualization of extruded shape before going to the

experiment. Punch displacement and maximum load of punch gives the idea to design the die and punch set up and experimental procedure, and they will guide the experimental tests. Total velocity flow for different extruded shapes are studied three dimensionally. A change in the die or punch alters the pressure required to extrude a given product. Effective stress, effective strain, stress mean, total velocity are analyzed to know the extrusion-forging process.

CHAPTER 4

*EXPERIMENTAL
ANALYSIS*

4.1 Introduction to experimental analysis

In the present investigation, experimental studies are carried out with a view to compare the experimental results with the finite element analysis obtained from commercially available FEM software. Experiments are performed on an INSTRON[®]600KN Universal testing machine (maximum capacity of 600kN) for extrusion-forging of round sections using flat dies. Commercially available aluminium is used for above mentioned purpose. A combined extrusion-forging setup for laboratory experimentation is designed and fabricated.

4.2 The test rig

The apparatus consists of six parts, namely; the container, the punch rod, the punch head with two different shape, the forging-extrusion die holder, support plate, a series forging-extrusion dies with different shape. The experimental setup used in the present analysis and series of test is shown in Figure 4.1. The details' lists of components for the combined extrusion-forging test rig are given in below in Table 4.1. The container (140mm diameter and 100mm length) is made of EN31 steel, and having a cylindrical chamber (50mm ϕ and 100mm length). This is accomplished first by turning the outer diameter and drilling the inner chamber (having tolerance of $\pm .02\text{mm}$) using wire cut EDM. The detail dimensions are given in Figure 4.2. To avoid back slip of the sleeve from the container during experimentation container cover plate (Figure 4.3) is used. Four numbers of Allen's screw holes are made on both flat faces. Inner faced holes are used for bolting the whole assembly and outer holes are used to hold firmly the cover plate. A container sleeve (Figure 4.4), insert for container, outer diameter match with the inner diameter of the container. The inner diameter of the sleeve matches the diameter of the punch rod. Its function is to guide the punch rod through it and avoid bulging of the punch rod. Similar processes are followed for manufacturing of the extrusion-forging die holder (Figure

4.5). Two punch rod; punch rod-1 with plate (Figure 4.6) and punch rod-2 (Figure 4.7) are made of D2 steel used for experiment. Two sets of punch head, square (Figure 4.8) and hexagon (Figure 4.9) are used for extrusion-forging. Punch heads are attached with the punch rod-2 by push fit arrangement. Figures 4.10 to 4.13 illustrate the circular die, circular split die, square and hexagon groove split die respectively with detail drawing. Base plate and support plate are made of EN8 steel are shown in Figure 4.14.

Table 4.1: List of components

SL. NO.	DESCRIPTION	QTY.	MATERIAL	SIZE	REMARK
1	COVER PLATE	1	EN8	Ø140×10	HRc 45-48
2	CONTAINER	1	EN31	Ø140×100	HRc 45-48
3	CONTAINER SLEEVE	1	EN31	Ø50×100	HRc 45-48
4	DIE HOLDER	1	EN31	Ø140×50	HRc 45-48
5	SUPPORT PLATE	1	EN8	Ø160×20	HRc 45-48
6	PUNCH ROD-1	1	D2	Ø30×150	HRc 50-55
7	PUNCH ROD-2	1	D2	Ø15×38	HRc 50-55
8	HEXAGON PUNCH HEAD	1	D2	4.5×4.5	HRc 50-55
9	SQUARE PUNCH HEAD	1	D2	6.36×6.36	HRc 50-55
10	SQUARE SPLIT DIE	01 Set	D2	5.65×5.65	HRc 50-55
11	HEXAGON SPLIT DIE	01 Set	D2	4×4	HRc 50-55
12	CIRCULAR SPLIT DIE	01 Set	D2	Ø50×4	HRc 50-55
13	CIRCULAR DIE	01 Set	D2	Ø50×37	HRc 50-55
14	BASE PLATE	1	EN8	Ø140×30	HRc 45-48
15	PUNCH PLATE	1	EN31	Ø160×20	HRc 45-48
16	COUNTER SHINK SCREW	4	EN31	M8×15	
17	ALLEN SCREW	1	EN31	M8×30	
18	ALLEN SCREW	4	EN31	M10×110	

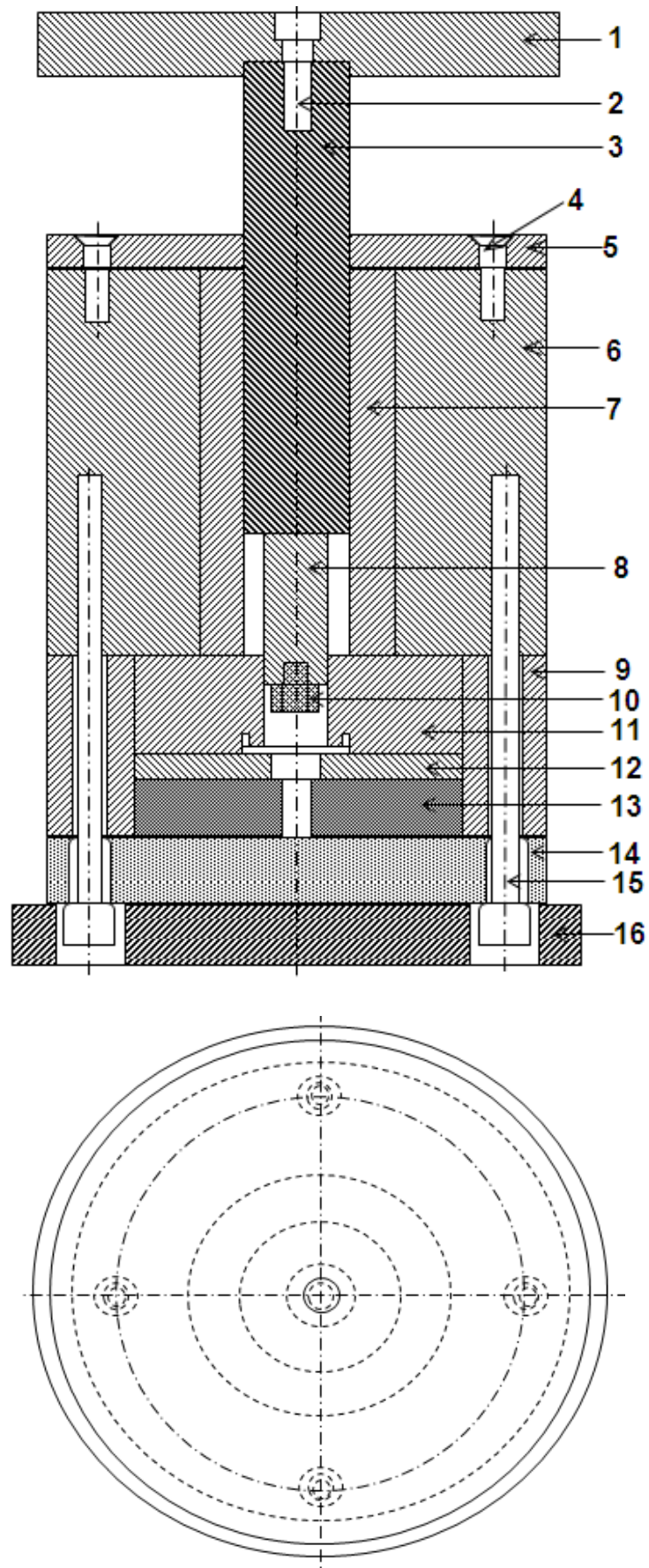


Figure 4.1 Extrusion-forging die set up assembly

Name of different components are as follows; 1-Punch plate, 2-Allen screw, 3-Punch rod 1, 4-Counter sink screw, 5-cover plate, 6-Container, 7-Container sleeve, 8-Punch rod 2, 9-Die holder, 10-Square and hexagonal punch head, 11-Circular die, 12-Circular split die, 13-Square and hexagonal grove split die, 14-Base plate, 15-Allen screw and 16-Support plate.

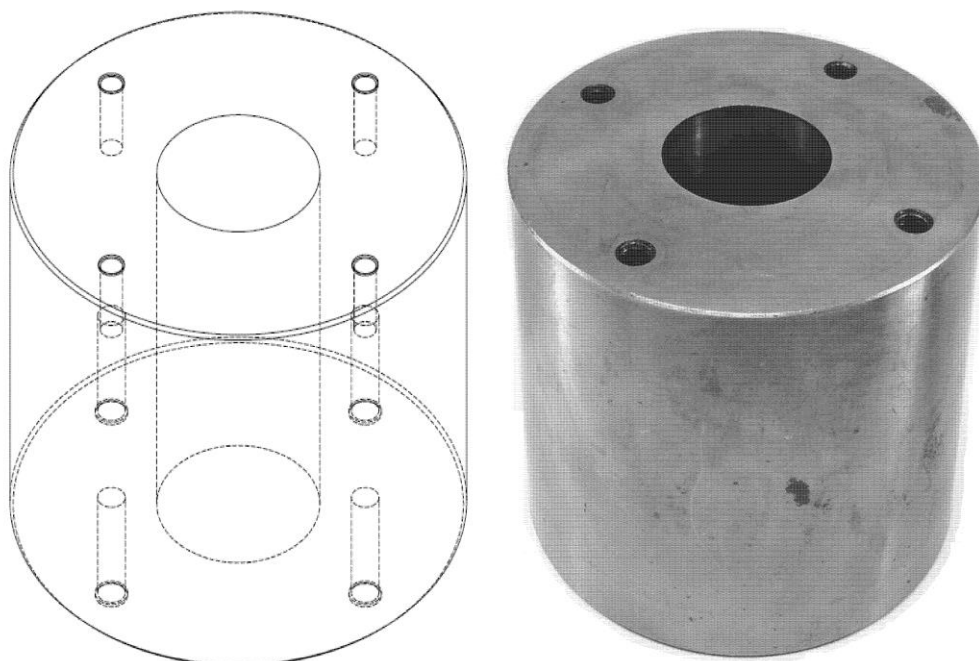
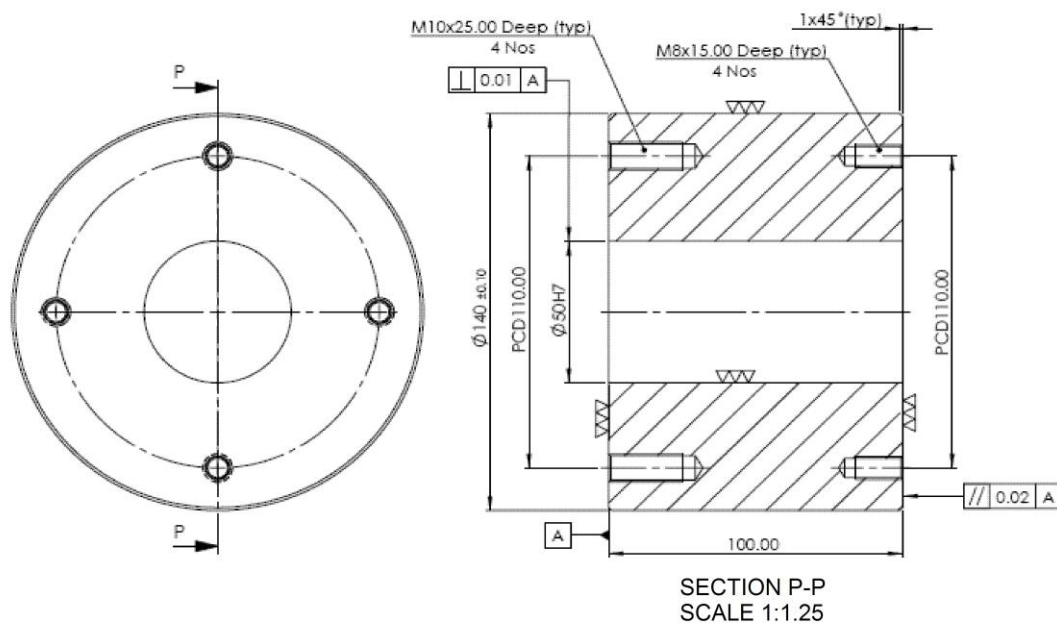


Figure 4.2 Container

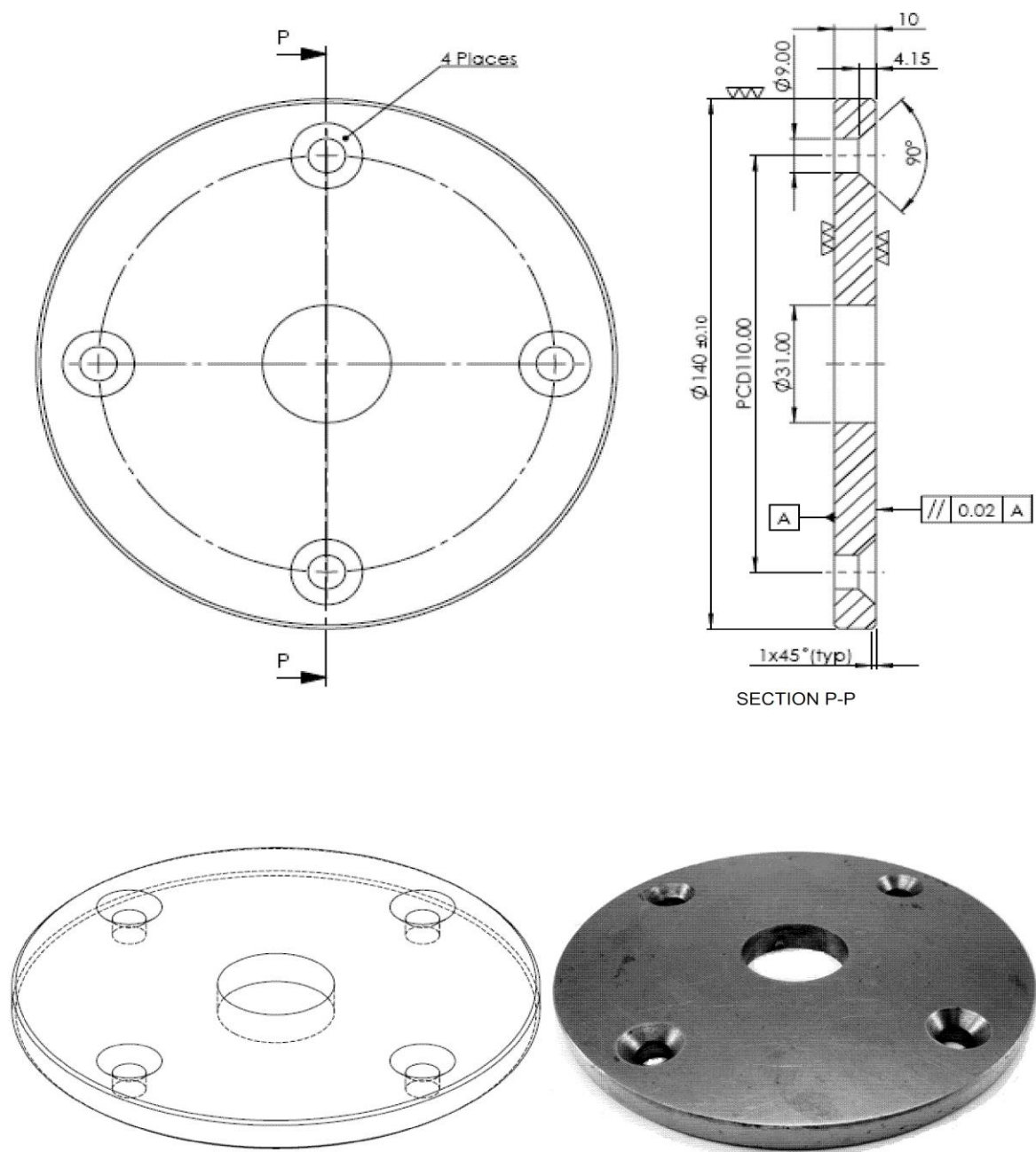


Figure 4.3 Cover plate for container

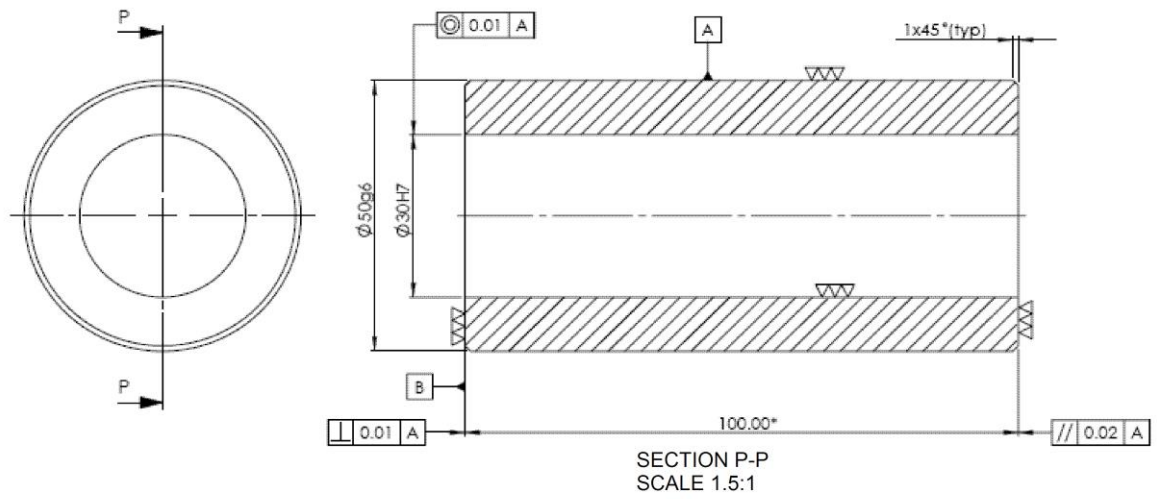


Figure 4.4 Sleeve

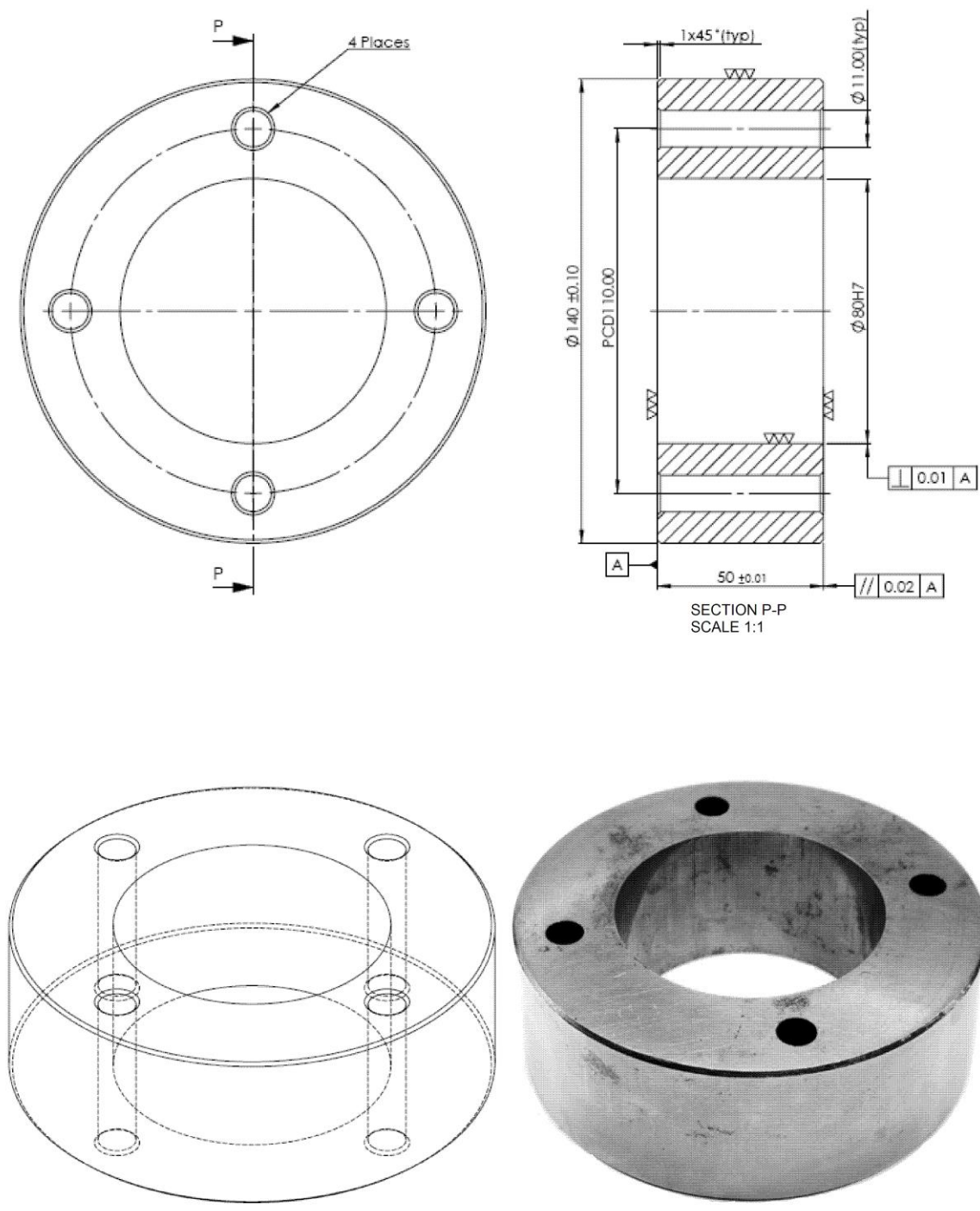


Figure 4.5 Extrusion forging die holder

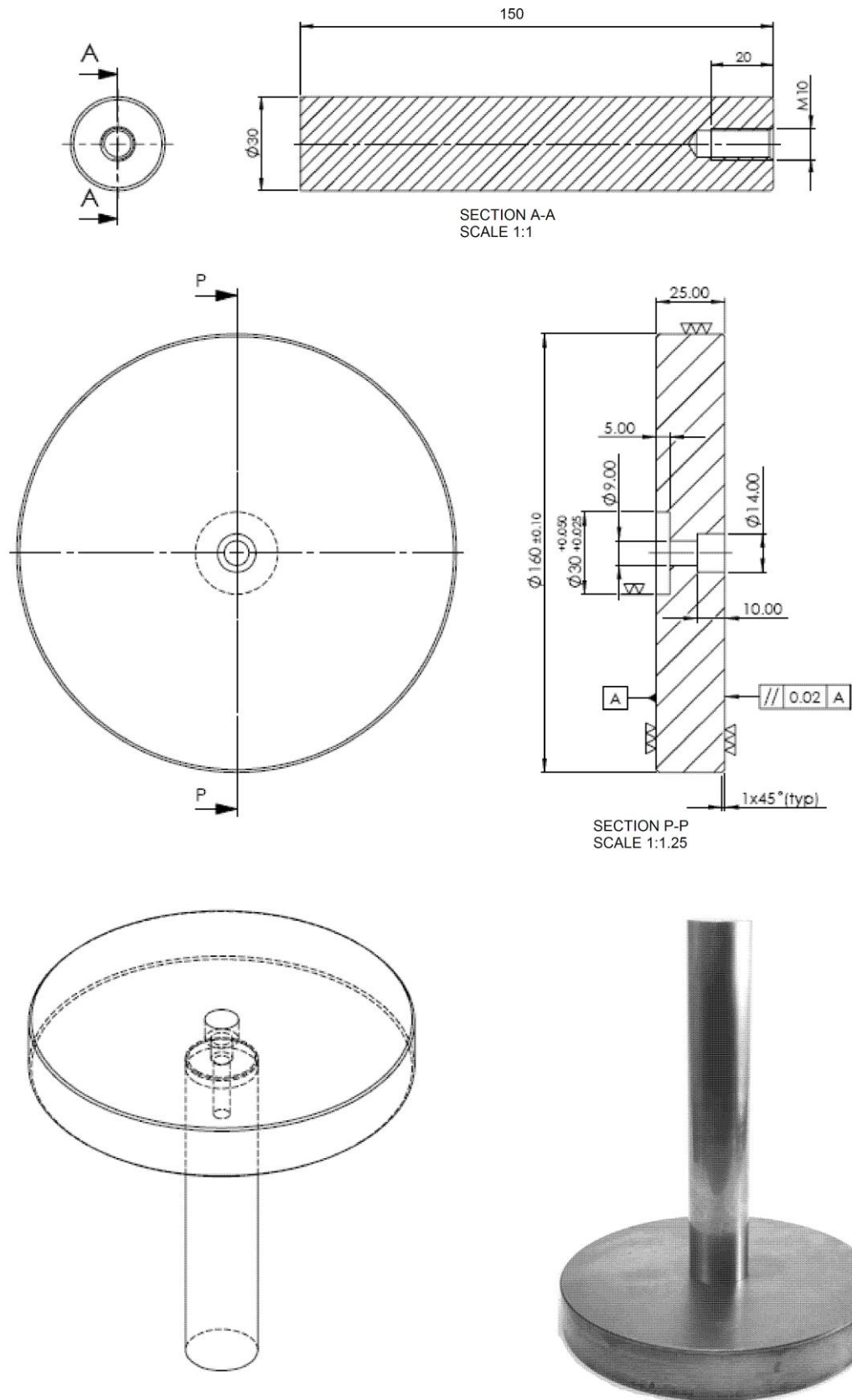


Figure 4.6 Punch with punch plate

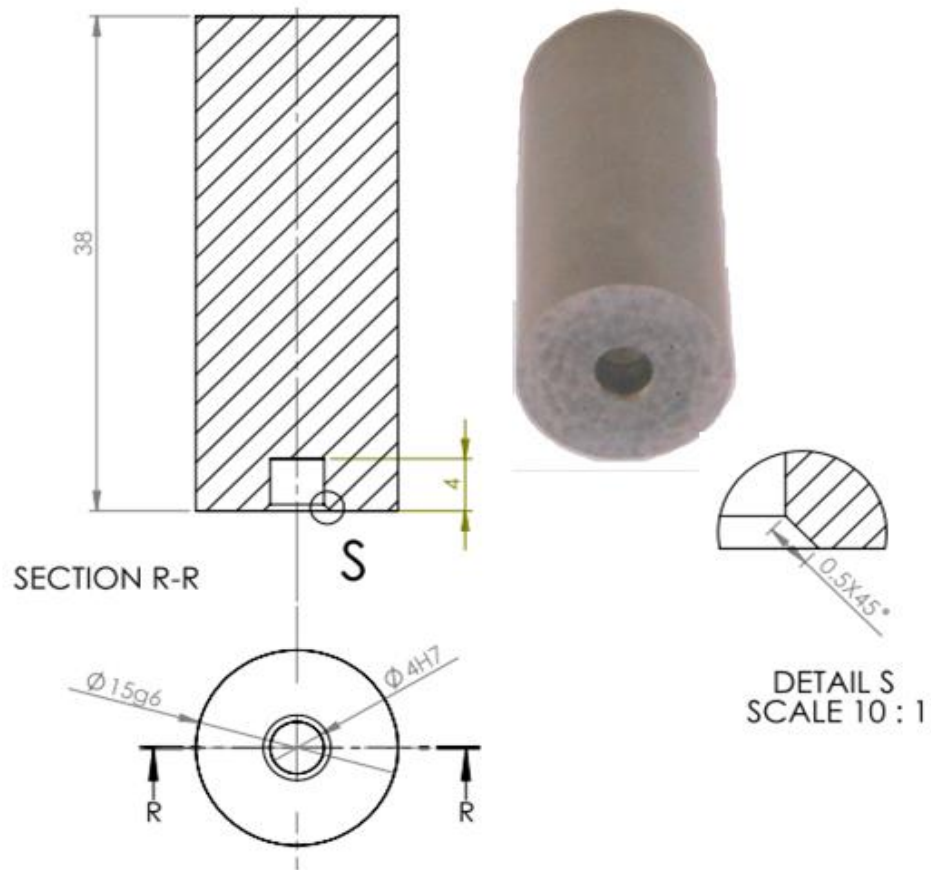


Figure 4.7 Punch rod 2

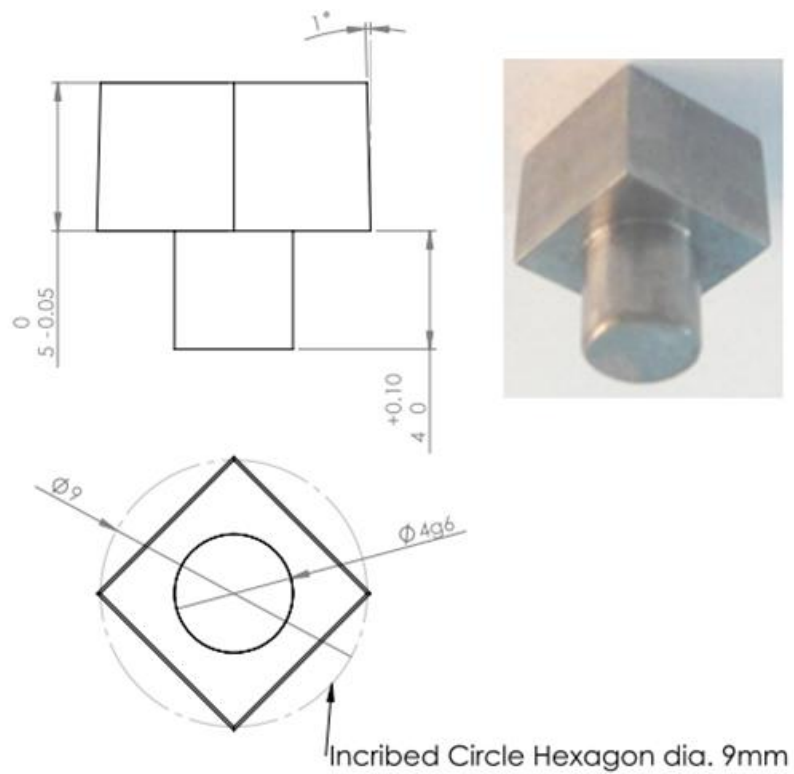


Figure 4.8 Square punch head

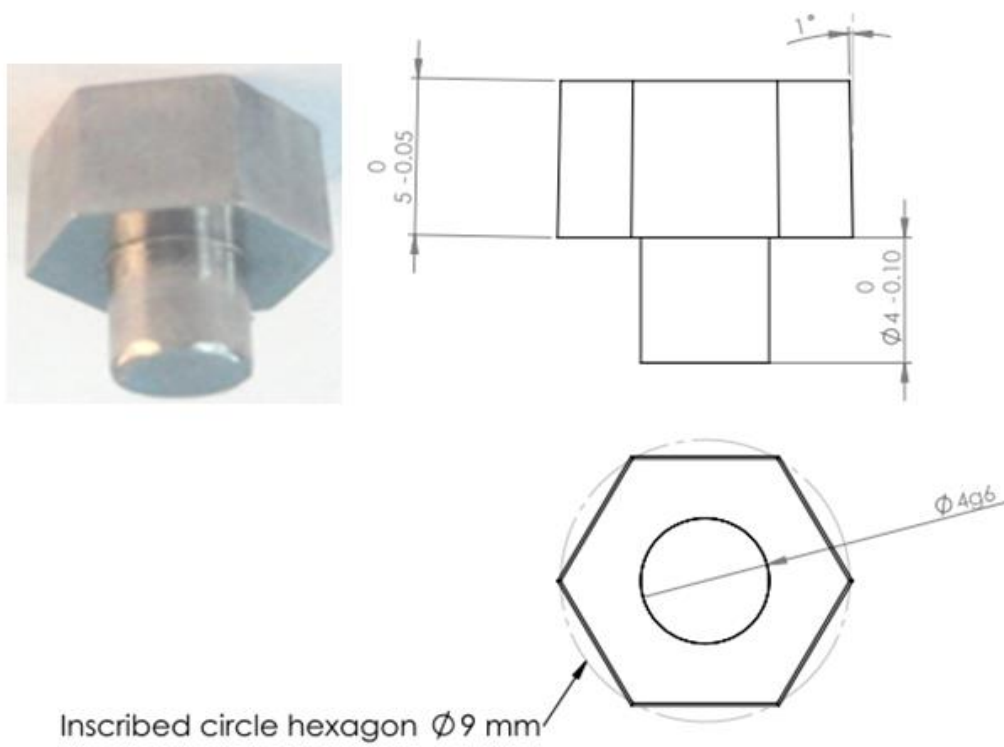


Figure 4.9 Hexagon punch head

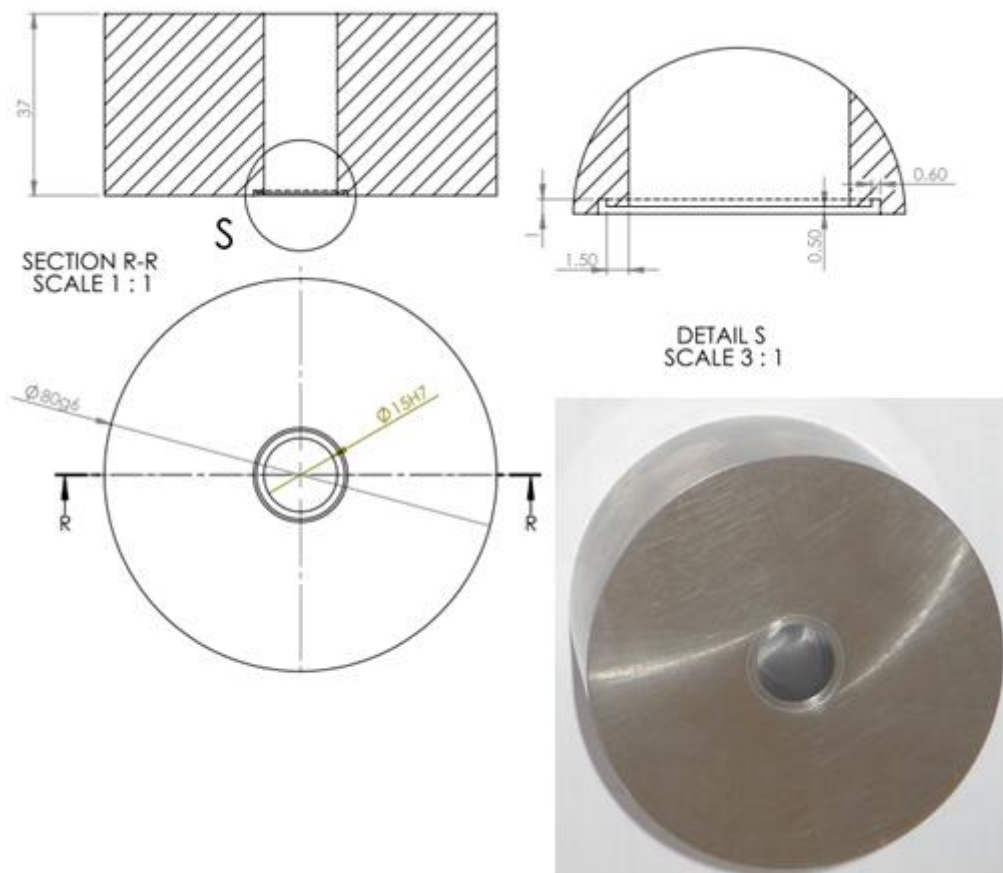


Figure 4.10 Circular die

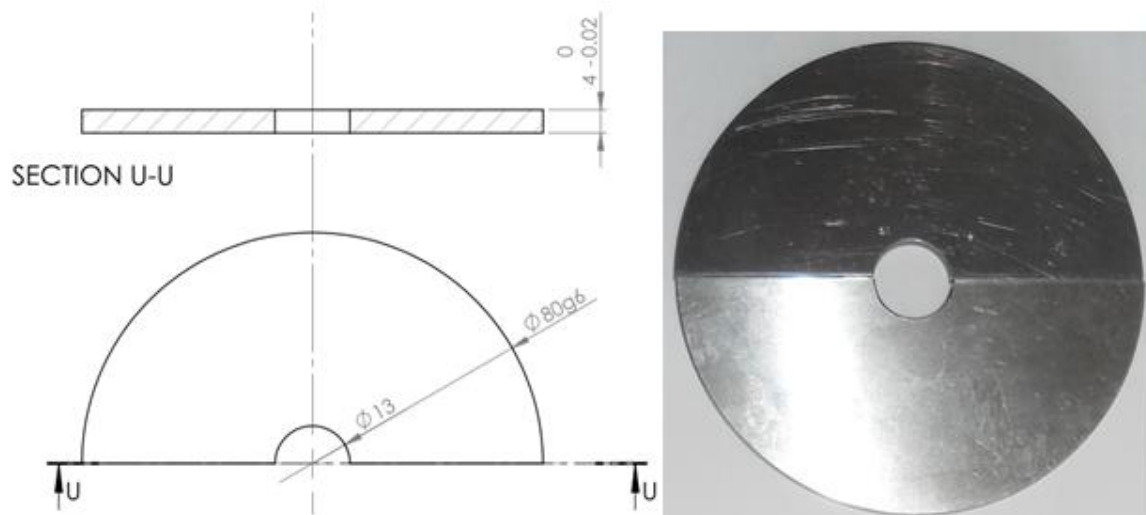


Figure 4.11 Circular split die

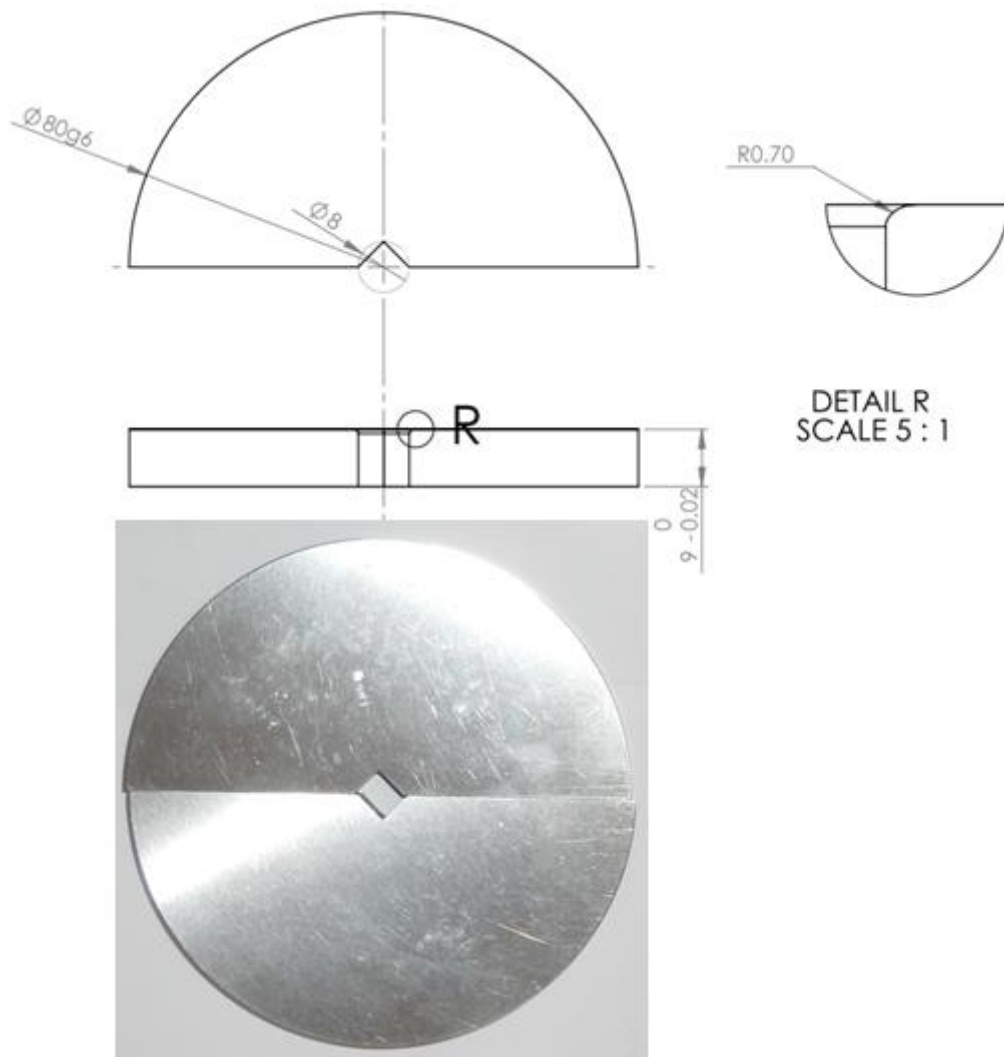


Figure 4.12 Square groove split die

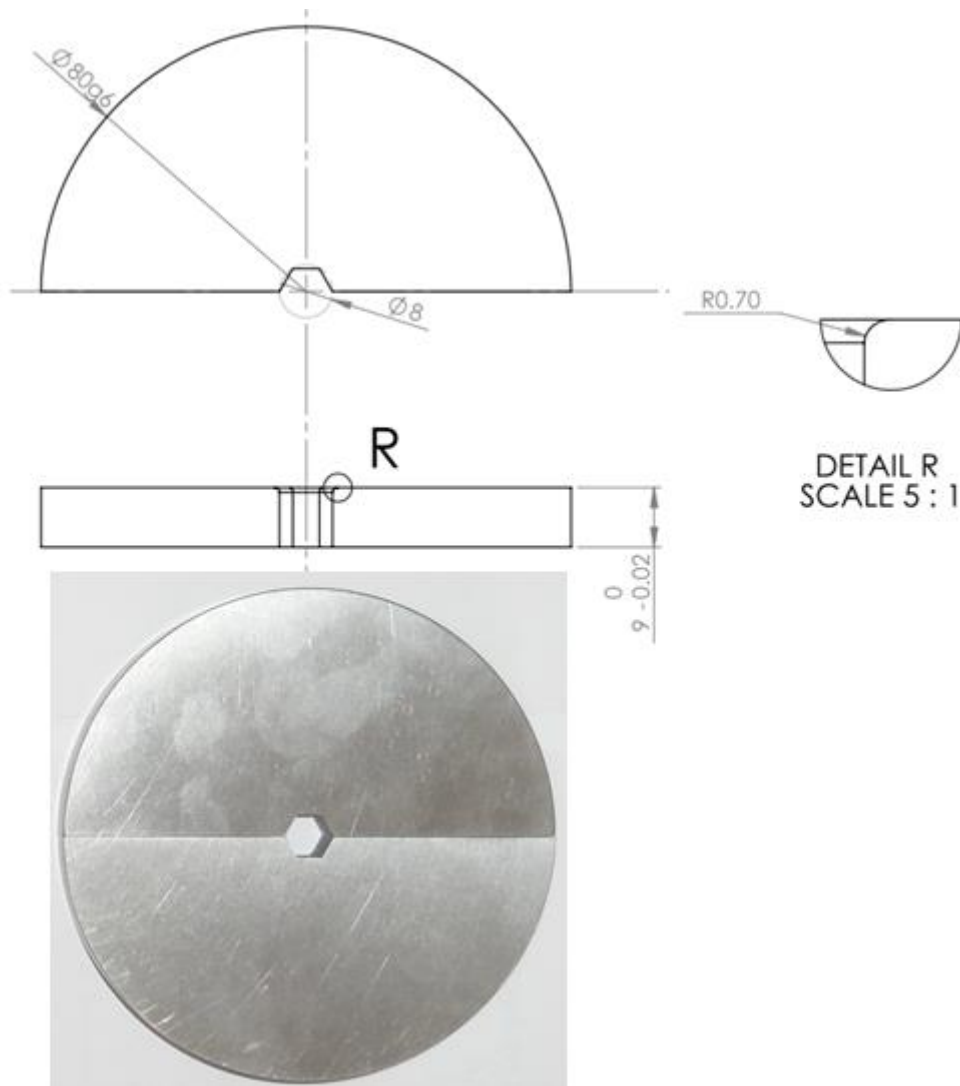


Figure 4.13 Hexagonal groove split die

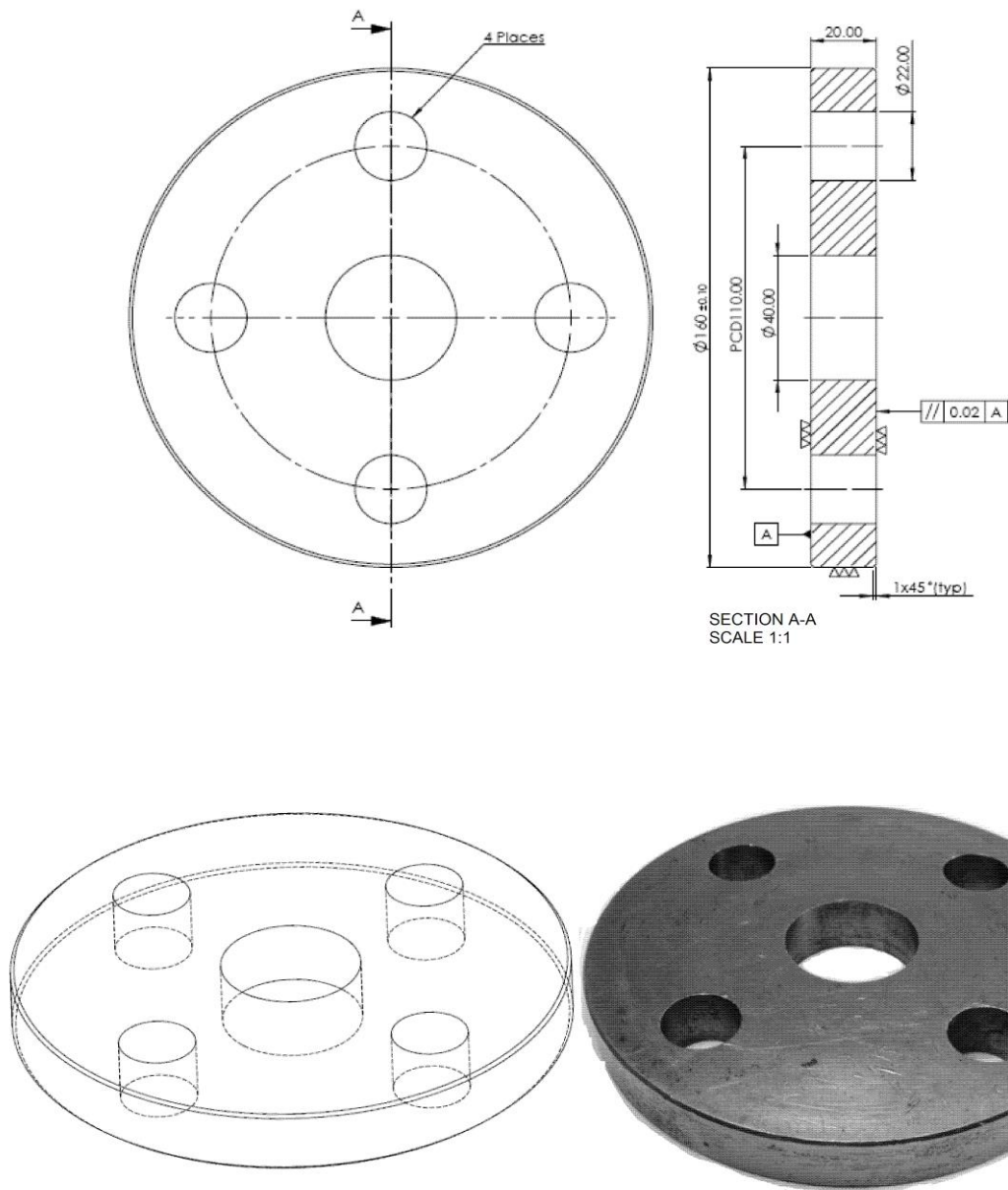


Figure 4.14 Base plate

4.3 Experimental set up and procedure

The die-sets, the extrusion-forging die holder and the inside face of the container and sleeve is cleaned with carbon tetrachloride before starting the tests to degrease the total setup. The two halves of the extrusion-forging die sets are then push fitted into the die holder. The inner surfaces of the dies and outer surfaces of the specimen are smeared lubricated using lithium based grease (commercially available SKF LGMT 3IN1 general purpose grease). The

prepared aluminium specimen is placed inside the cavity of the extrusion-forging die and the total assembly is perfectly made by screwing the four alloy's bolts. The specimen is so placed inside the extrusion-forging die cavity so that the axis of the billet coincides on the assembled setup axis and machine axis. The full assembly is then placed on the lower table of the universal testing machine (INSTRON® 600KN) as shown in Figure 4.15, having maximum capacity of 600kN. The punch is then inserted into its position. After centering the apparatus under the machine lower table, the machine is started and the extrusion-forging process is continued. To avoid rate affect the movement of the punch being adjusted to 1 mm per minute. Punch load is recorded at every 30sec of punch travel. Combined extrusion-forging is continued until the specified punch movement reaches to produce the desired shape (male/female socket adopter). At this point, the machine is stopped, and the test is terminated.

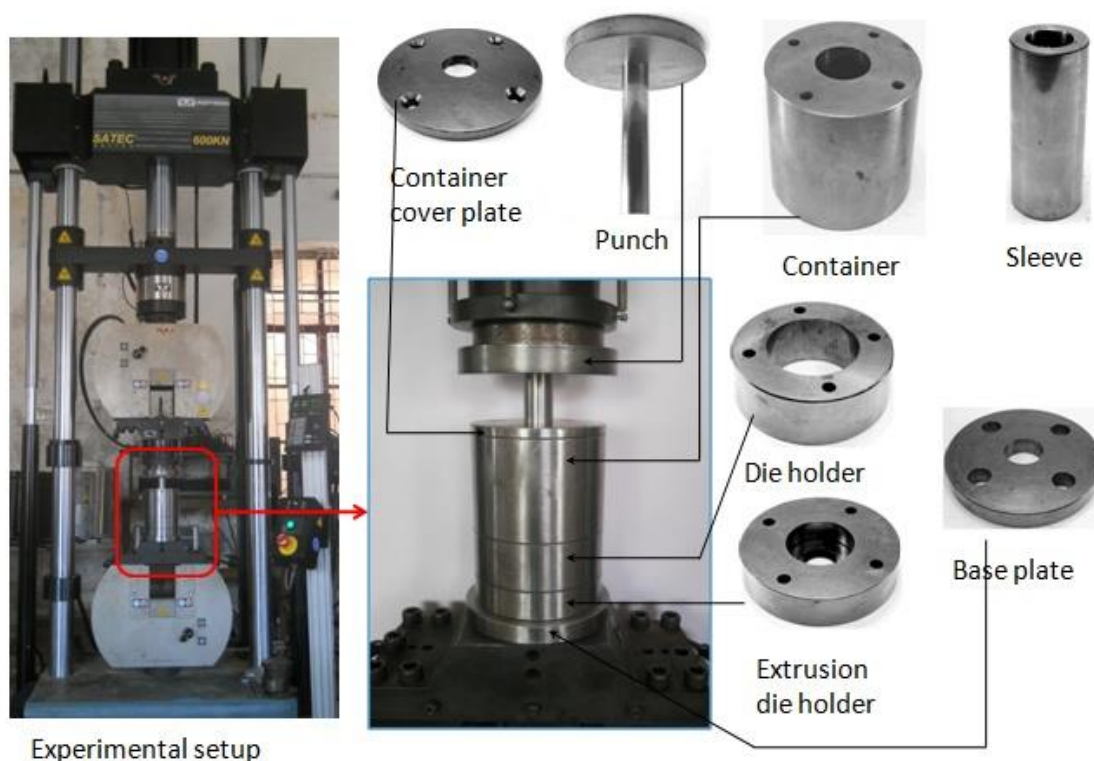


Figure 4.15 Photographic view of experimental set up with main components

The die holder is separated from the extrusion chamber after the experiment, and finally the die halves with the extruded product are pressed out from the die holder. Experiments were conducted for different types of socket adopter and for various punch movement. The photographic view of all the products are discussed and shown in Chapter 5 for combined extrusion-forging process.

4.4 Determination of stress-strain characteristic of aluminium

In order to plot the stress-strain diagram, a cylindrical specimen of aluminium of 21.75 mm diameter and 37.32 mm length is machined from casted billet. The specimen had oil grooves turned on both ends to entrap lubricant during the compression process. Its ends were adequately lubricated with grease and tested in uniaxial compression on the INSTRON®- 600KN hydraulic pressing machine (Figure 4.16). The compression rate is 1mm/min, is same that adopted for extrusion test. The compressive load is recorded at every 0.5 mm of punch travel. After compressing the specimen to about 5 mm, it was taken out from the sub-press, re-machined to the cylindrical shape of diameter 37.32mm with the oil grooves again turned on both ends and tested in compression. This process continues until the specimen was reduced to about 17.32 mm. The stress-strain diagram of aluminium obtained in this manner is shown in Figure 4.17.

To determine the uniaxial yield stress we use a fitting curve of power equation with strength coefficient (K) 310MPa and strain hardening exponent (n) 0.12 as shown in Equation 1.

$$\sigma = 310 \times \epsilon^{0.12} \quad (4.1)$$

Obtained yield strength from stress-strain curve is 282MPa, and the power equation used for simulation analysis.

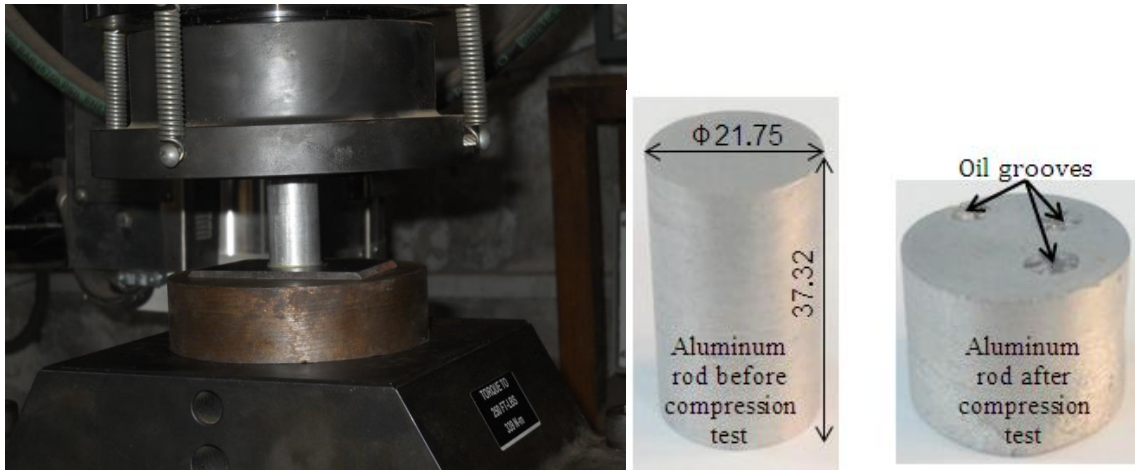


Figure 4.16 Compression test set up with aluminum specimen

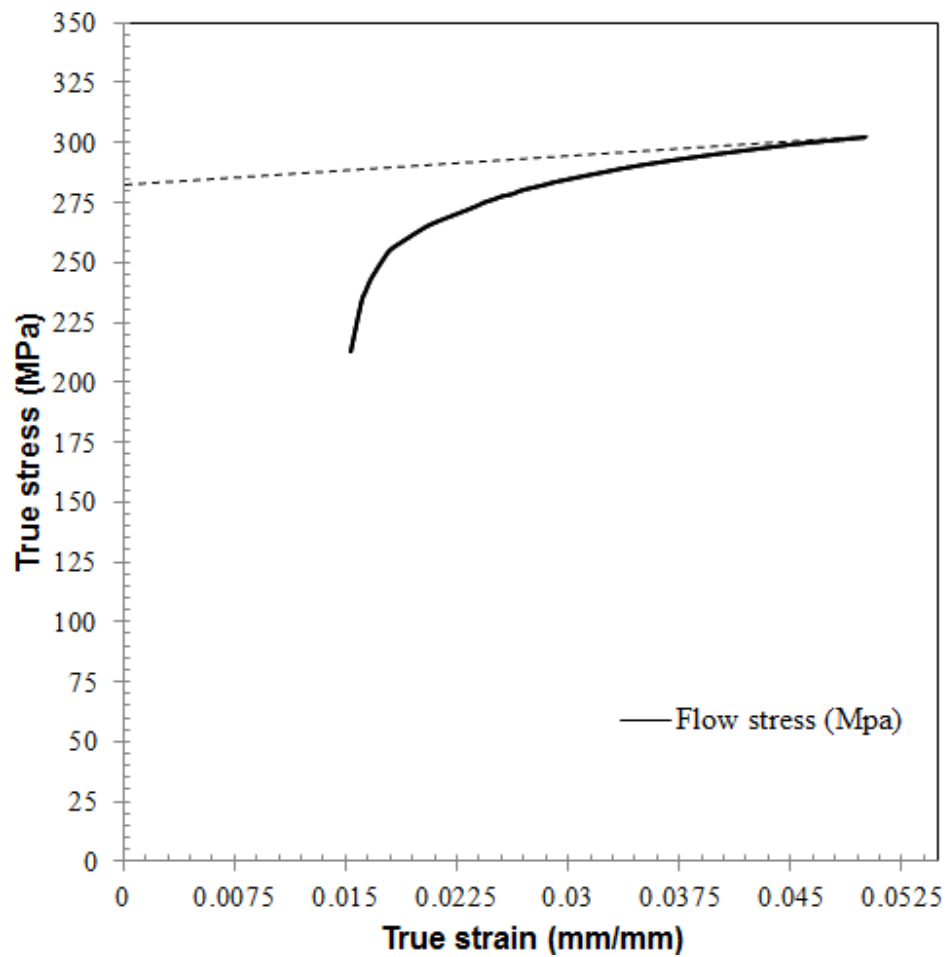


Figure 4.17 Stress-strain curves for aluminium

4.5 Determination of friction factor

In the metal forming process friction plays an important role. The metal flow is caused by the pressure transmitted from the dies to the deforming work piece. Therefore, the friction condition at the material/die interface greatly influences metal flow. In our experimentation, experiments are carried out at the lubricated condition. In this ring test, a flat ring shape specimen having OD: ID: Thickness ratios 6:3:2 is considered. The dimensions of the ring used are 22:11:7.3 mm. To estimate accurate friction between die inner surface and the billet material two flat plates (Figure 4.18) having the same surface condition that of internal surface of dies are equipped.

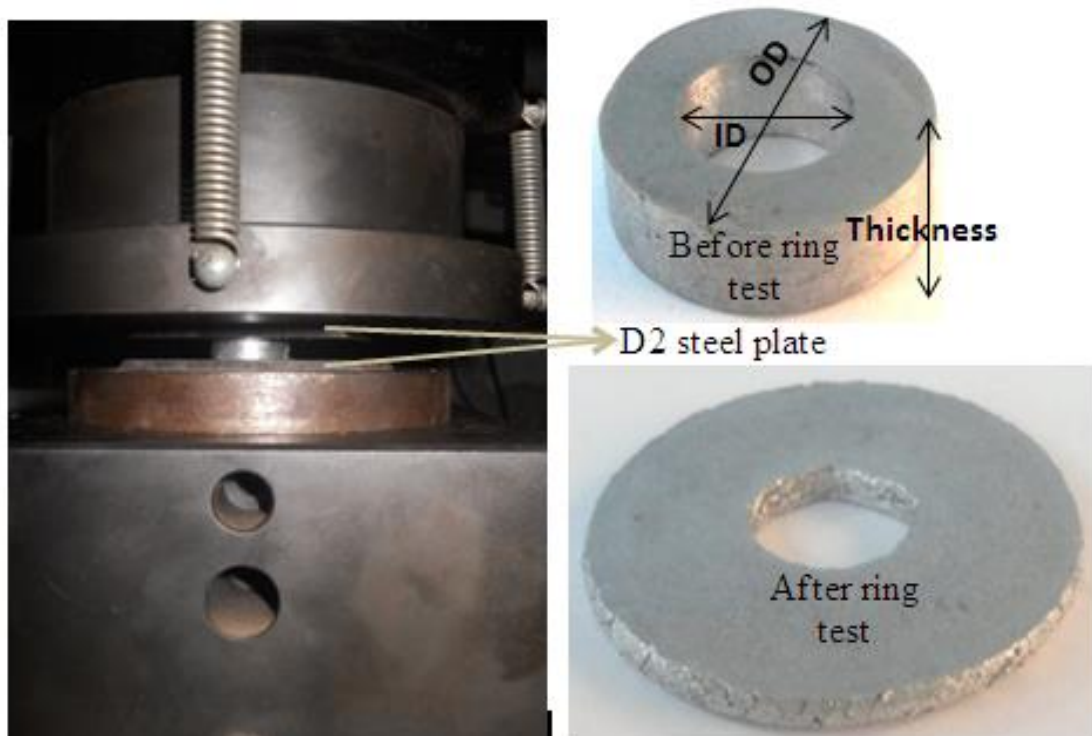


Figure 4.18 Set up for Ring test

To obtain the magnitude of the friction factors, the internal diameter of the compressed ring must be compared with the various available standard theoretical calibration curve of the friction factors, m . From the Figure 4.19, we found that for lubricated condition,

friction factor is 0.156. In FEA, we use this friction factor taken as one input parameter for simulation analysis.

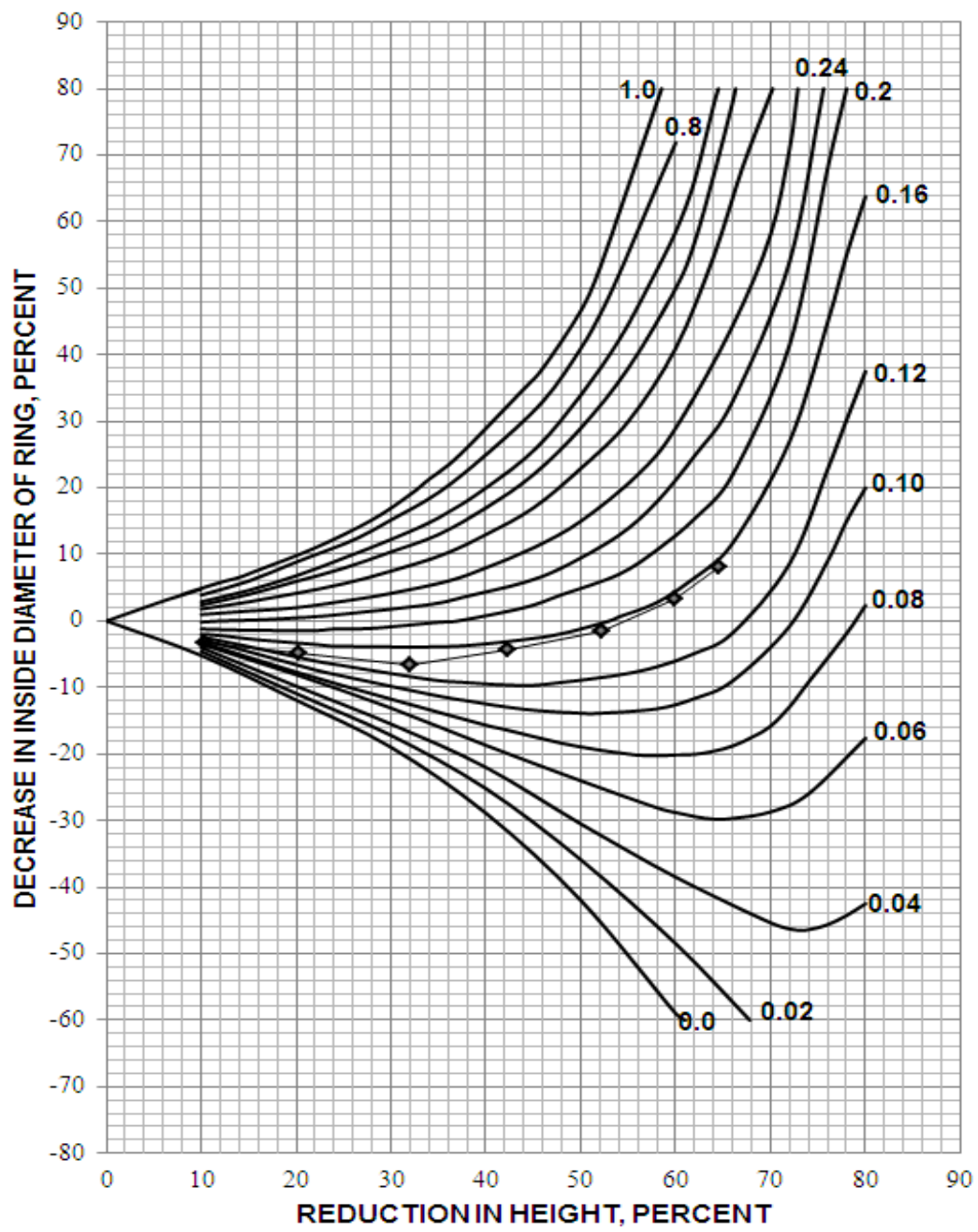


Figure 4.19 Theoretical calibration curve for standard ring (6:3:2)

4.6 Result analysis

4.6.1 Variation of punch load with punch stroke from experiment

Experiments are carried out for combined extrusion forging process. Referring to the Figure 4.20, it is seen that the whole process consists of four major stages: namely (i) a coining stage in which initial compression of the billet takes place. (ii) The second stage refers to the

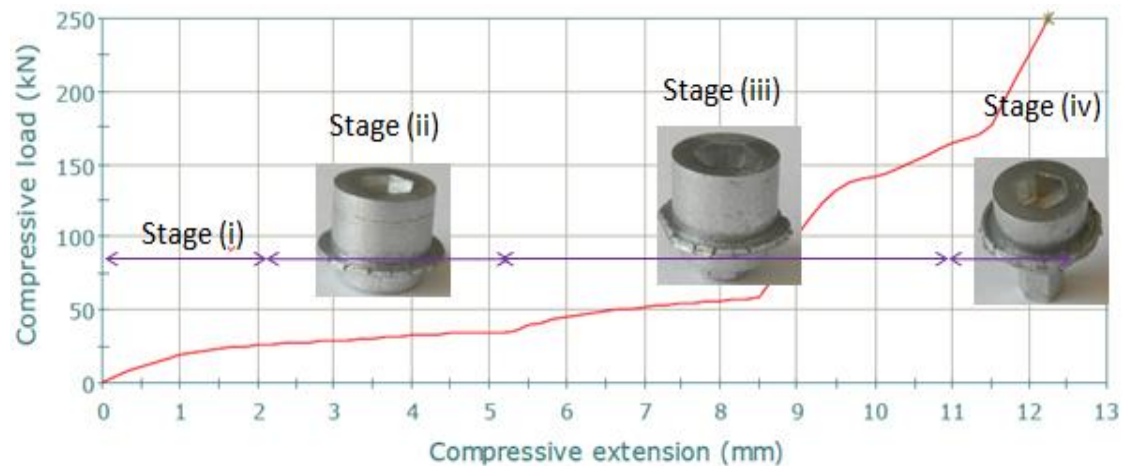


Figure 4.20 Various stages of combined extrusion-forging process

combined extrusion-forging stage where the billet forged till it touches the die wall and partly extruded. In this stage load increase slowly with respect to punch movement. (iii) In the third stage punch takes the high load to start the extrusion. Steady state extrusion takes place in next to the third stage. (iv) in fourth stage Flash begins and final forging take place with high punch load. Figure 4.21-4.24 represents the variation of punch load with punch movement for four different types of socket adopter.

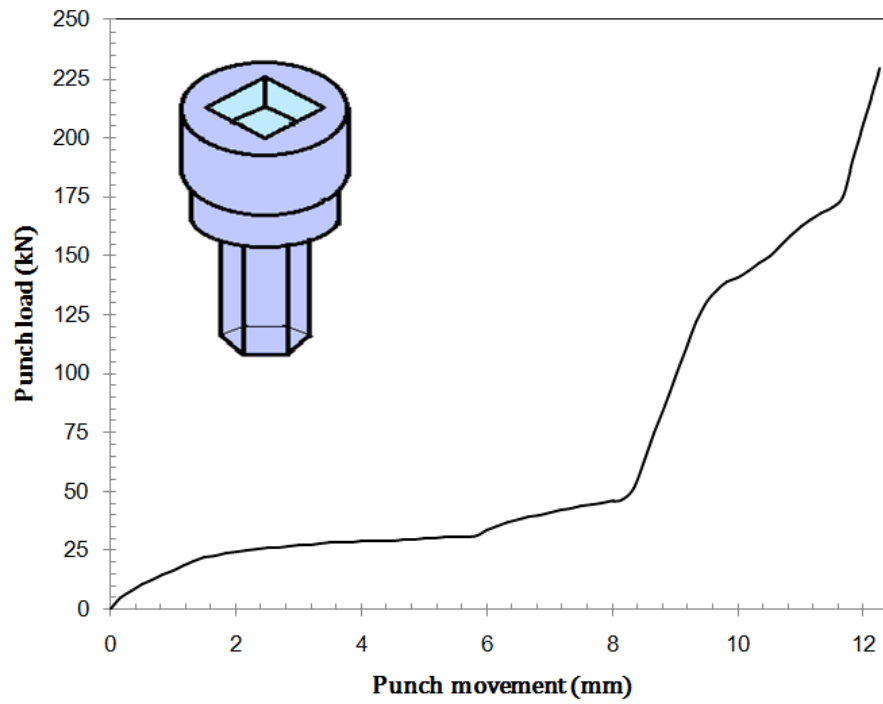


Figure 4.21 Variation of load with stroke for square-hexagon socket adopter

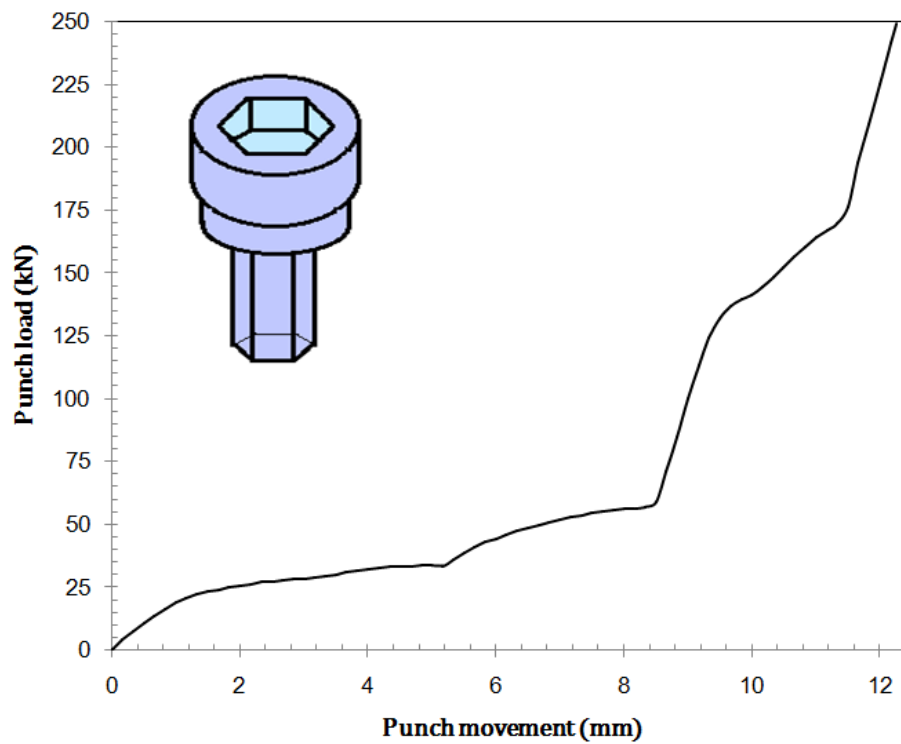


Figure 4.22 Variation of load with stroke for hexagon-hexagon socket adopter

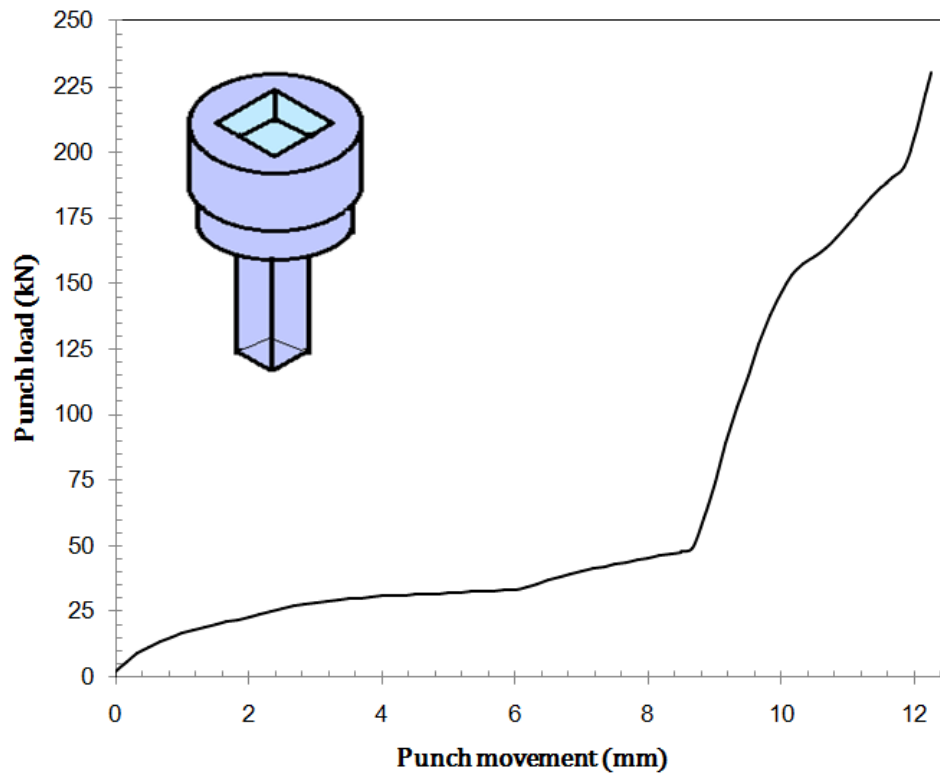


Figure 4.23 Variation of load with stroke for square-square socket adopter

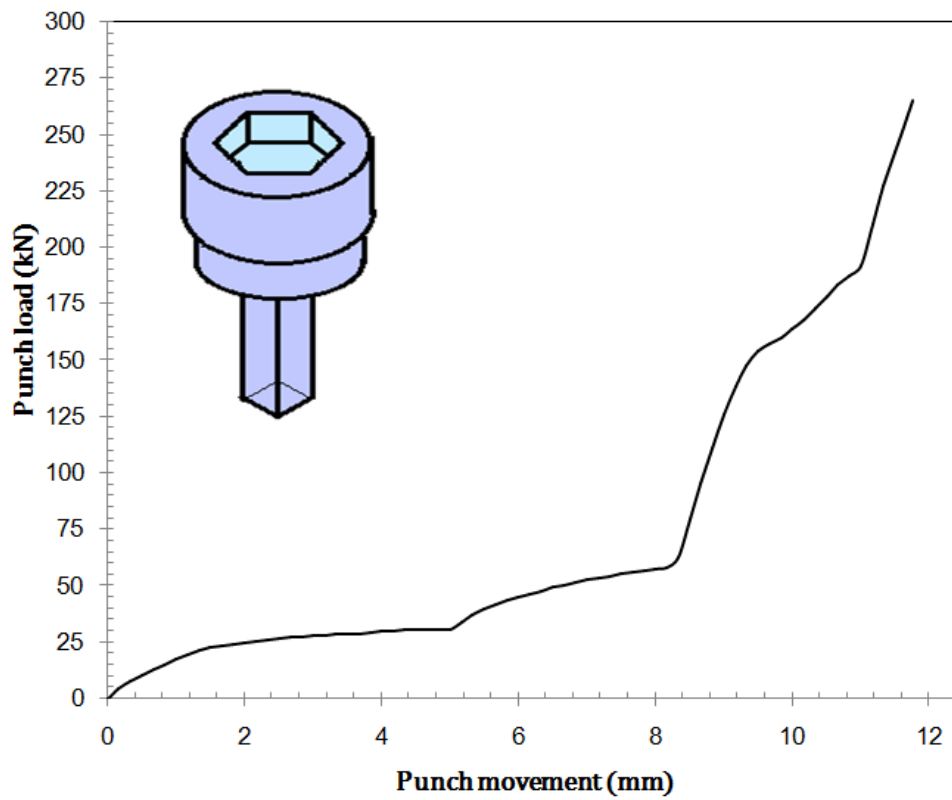


Figure 4.24 Variation of load with stroke for hexagon-square socket adopter

4.6.2 Micro hardness and distortion of grain boundary

Vicker micro hardness testing instrument is used for the measurement of micro hardness of extruded-forging aluminium material at different zones. Before measurement, setting parameter is taken as load of 100gf with 10second dwell time. Micro hardness is measured along the line from centre line to outwards, called as zone I at top portion and zone II at towards the bottom portion of the socket as shown in Figure 4.25. Zone III is taken along the centre line. Along the centre line the hardness values are quietly linearly distributed (Figure 4.28). But in zone I (Figure 4.26) and zone II (Figure 4.27), the effect of micro hardness has lightly significant.

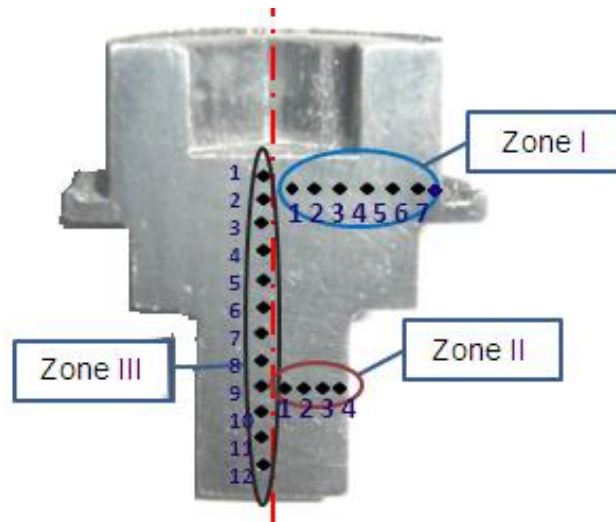


Figure 4.25 Different zones for measurement of micro hard ness

Zone I indicates the forging zone, where the hardness decreases towards the outward or wall of container form centre (from position 1 to 7). This is due to the present of dead metal zone towards the container wall. The element at dead metal zone has lo low strain harden as compare to the element at deform zone.

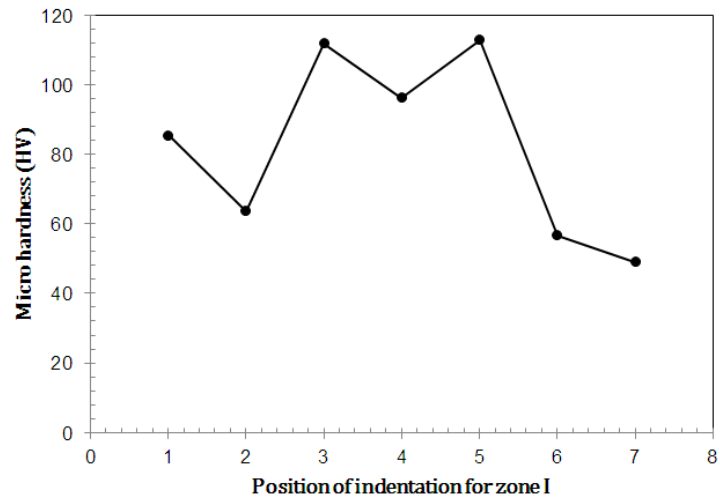


Figure 4.26 Distribution of micro hardness at zone I

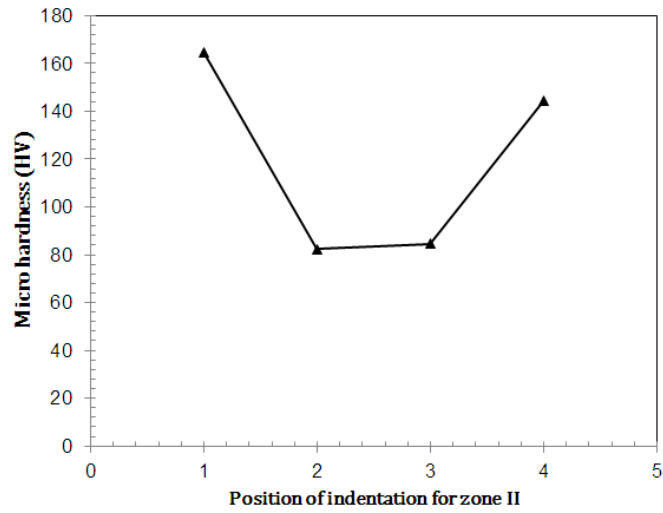


Figure 4.27 Distribution of micro hardness at zone II

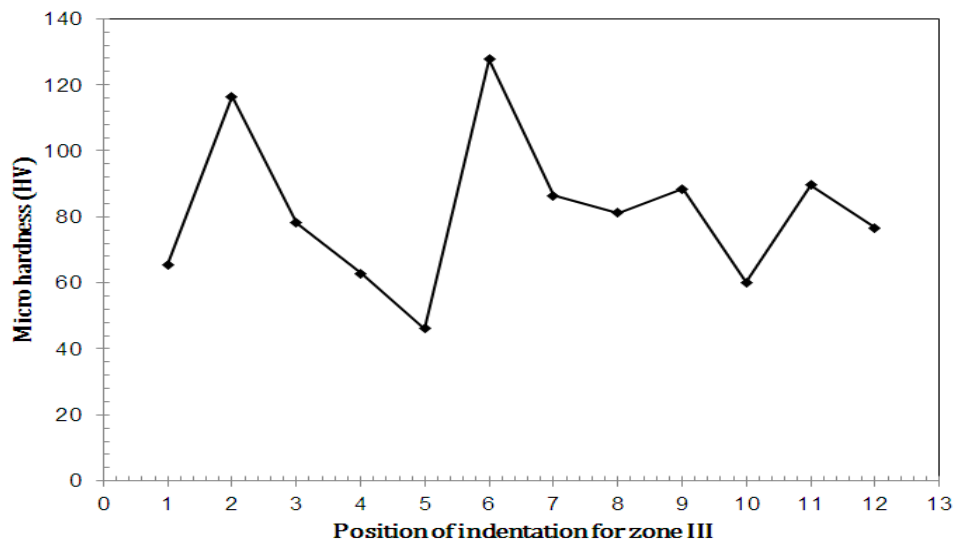
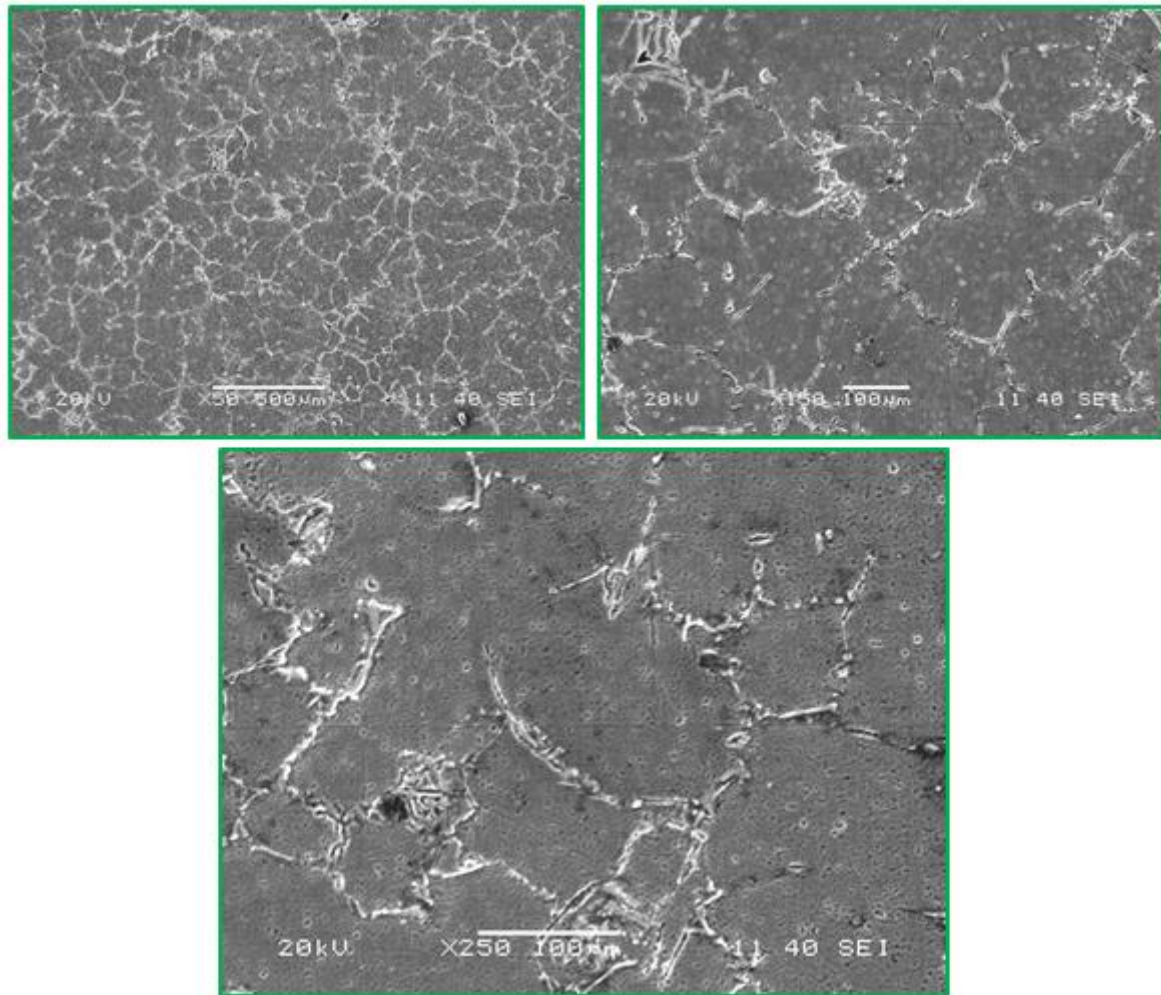


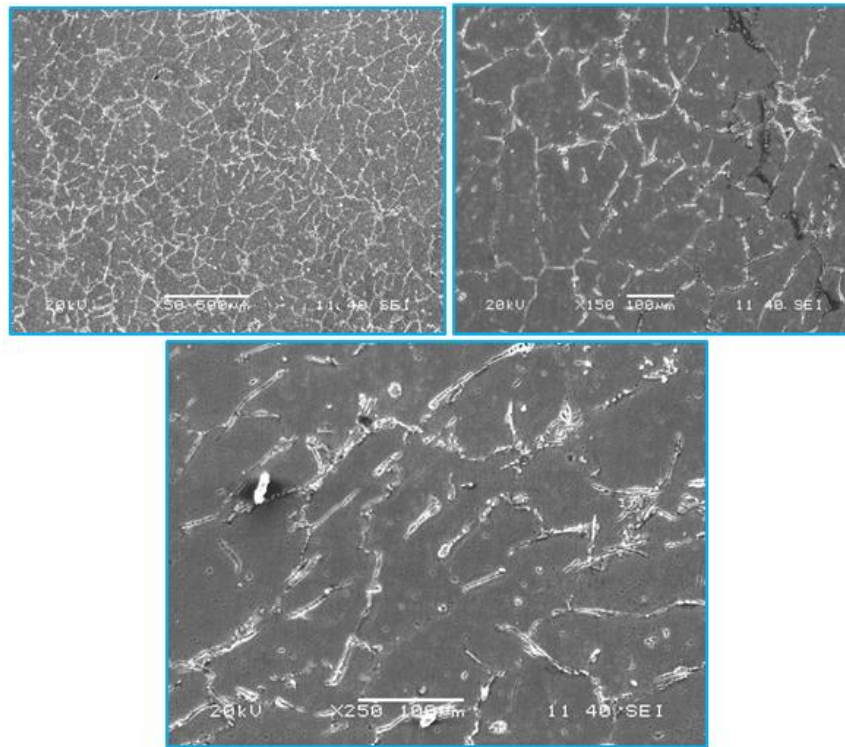
Figure 4.28 Distribution of micro hardness at zone III

To study the microstructure in terms of view of grain boundary of aluminium before and after combined extrusion-forging, SEM is carried in JEOL (JSM.6480LV) scanning electron microscope. Due to extrusion forging, distortions of grain boundary are shown in Figure 4.29.

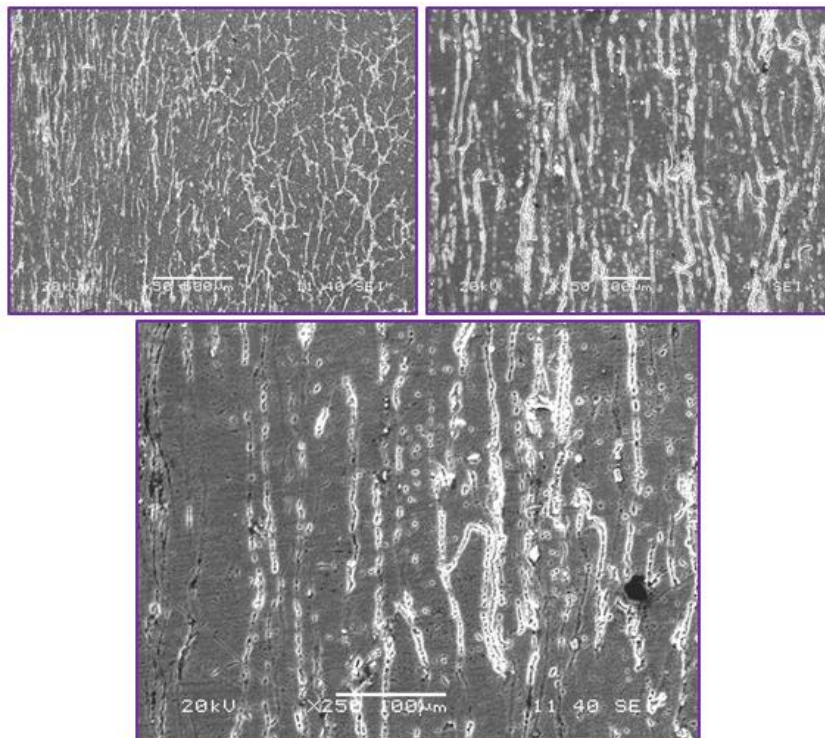


(a) Grain boundary of aluminium at different magnification before extrusion-forging process

Grain Boundaries are more restoring from oval to line structure after extrusion forging process. So, there is a change in grain boundary as the metal flow occurs.



(b) Grain boundary of aluminium at different magnification for intermediate stage of extrusion-forging process



(c) Grain boundary of aluminium at different magnification after extrusion-forging process

Figure 4.29 (a), (b) and (c); Grain structure of aluminium during extrusion forging process

4.5 Conclusions

We found that, the variation of load with punch stroke state four stages of combined extrusion-forging process. From hardness test it is concluded that at zone I, i.e along the centre line the micro hardness of metal is uniform. At zone II, micro hardness value decrease from centre line to outward. It is because the strain hardening is less at out ward due the presence of dead metal zone. Hardness depends upon the effective strain rate. In extrusion-forging process orientation of grains are occurred and affected by material properties. Grain boundary changes during this process were closely related to plastic strain.

CHAPTER 5

*COMPARISON OF RESULTS
AND
DISCUSSION*

5.1 Comparison of results

5.1.1 Peak loads of combined extrusion-forging process

Comparison of peak values of punch load both for simulation and experiment are presented in Table 5.1. The difference between FEA and experiment value for peak load are within 7.5%.

Table 5.1 Comparison of peak loads of combined extrusion forging process of four different types of socket adopter

Types of socket adopter	Simulation peak load (kN)	Experiment peak load (kN)	Absolute percentage error
Square-hexagon adopter	242.660	229.089	5.924
Hexagon-hexagon adopter	254.594	249.420	2.074
Square-square adopter	247.427	230.279	7.443
Hexagon-square adopter	281.7655	265.119	6.27

5.1.2 Deformed shape

Experiment and simulation are carried out by using same input parameters like punch speed, friction factor (in case of experiment lubricant is used) and strain rate. Socket adopter produced from simulation and experiment is shown in Figure 5.1. At different punch movement the die filling or product shape both for simulation and experiment are shown in Figure 5.2. Since the process is a extrusion-forging, at end of process only forging take place, hence as per the required design flash gutter arrangement is provide to take care of extra material [43]. The flash gutter is shown in Figure 5.3.

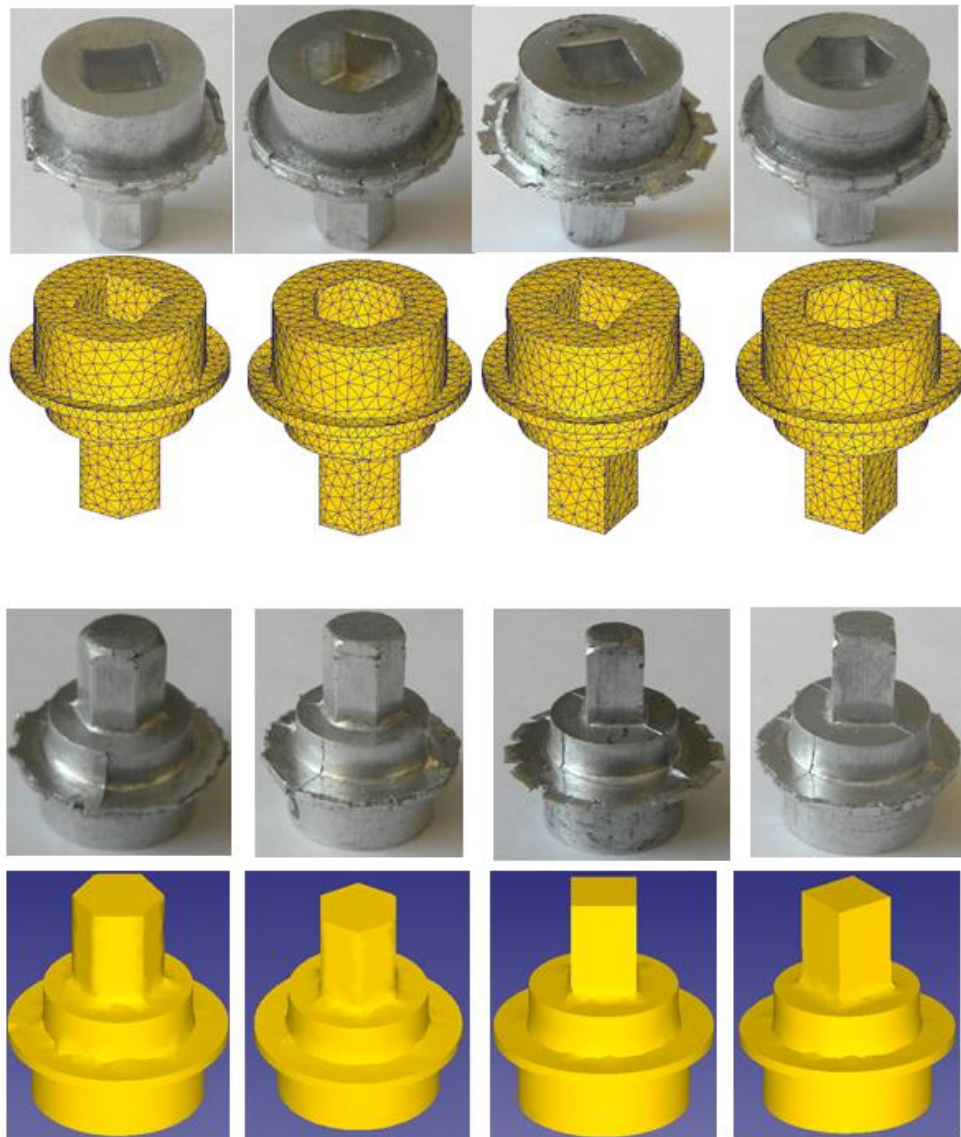
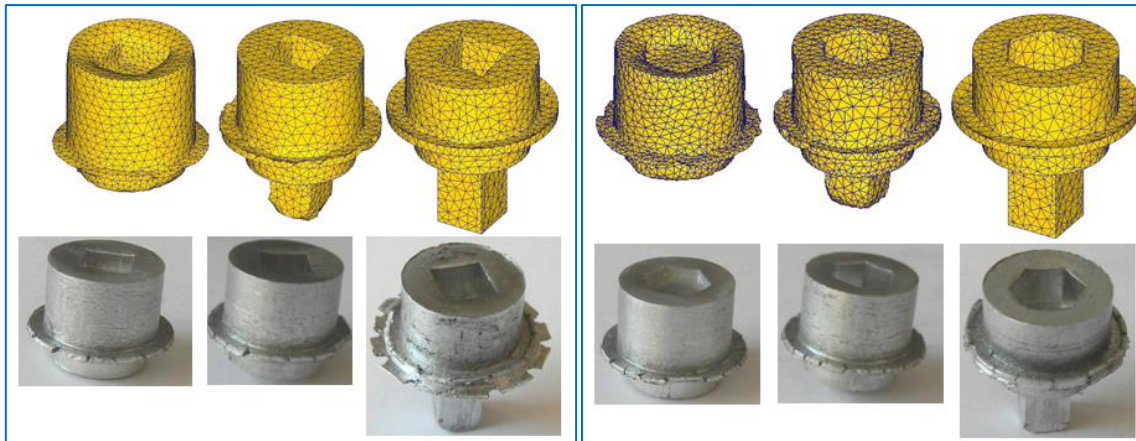


Figure 5.1 Extrusion-forging shapes for four types of socket adopter



(a) Square-hexagon socket adopter

(b) Hexagon-hexagon socket adopter



(c) Square-square socket adopter

(d) Hexagon-square socket adopter

Figure 5.2 Die filling at different punch movement for four types of socket adopter

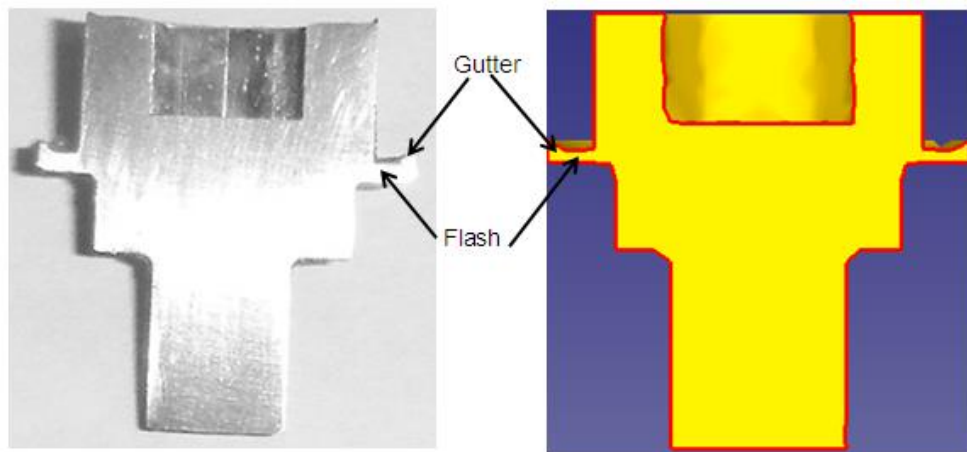
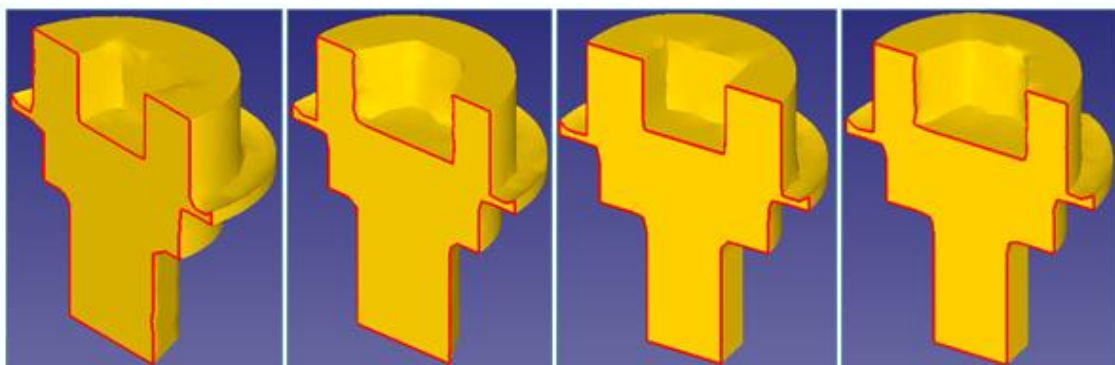
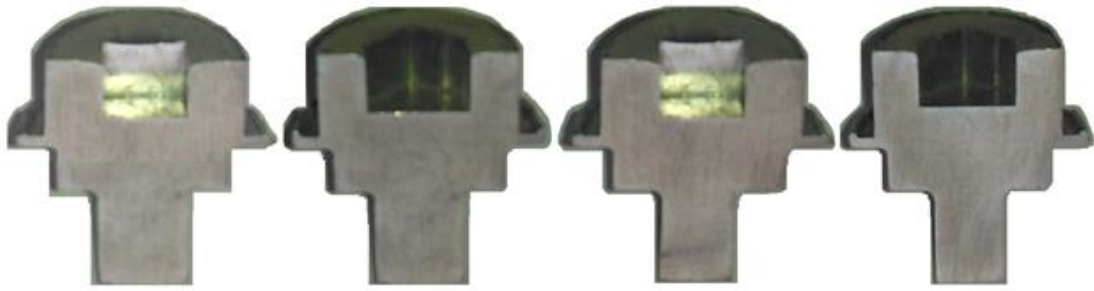


Figure 5.3 Flash gutter arrangements

Sectional view of socket adopter from experiment and simulation is shown in Figure 5.4.



(a) Sectional view (simulation)

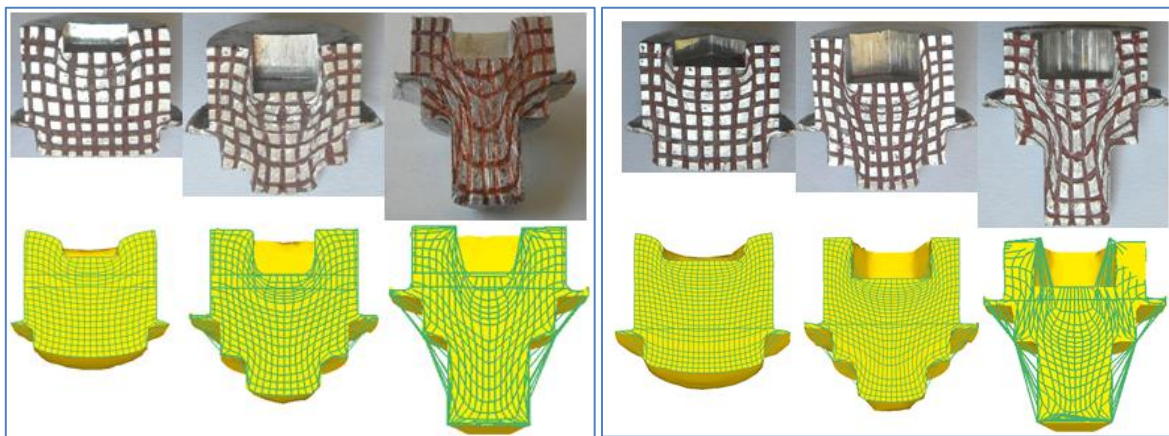


(b) Sectional view (experiment)

Figure 5.4 Sectional view of Socket adapter

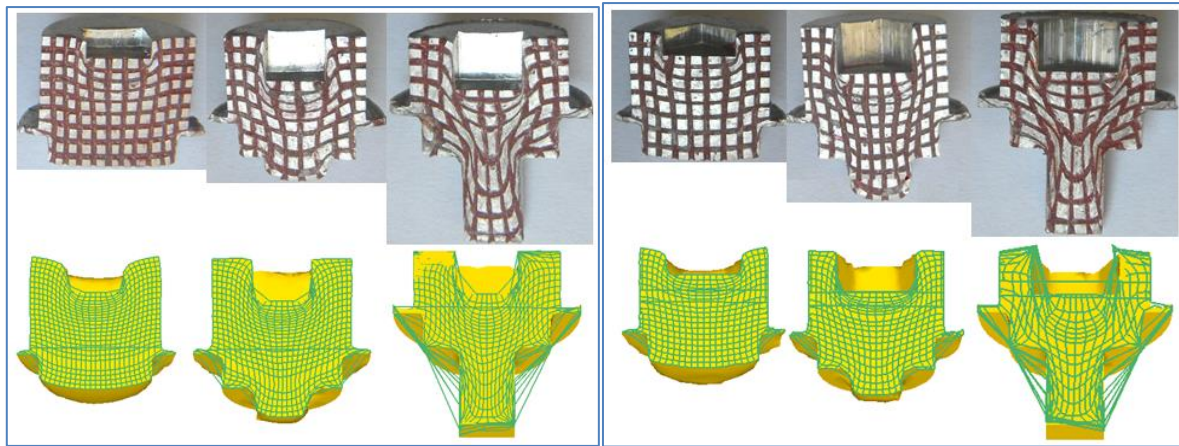
5.1.3 Metal flow pattern

As an illustration, Figure 5.5 shows the photograph of the show pattern at different punch movement of combined extrusion-forging process for both in FEM analysis and experimental investigation. The grid line distortion indicates that the process utilizes the maximum amount of redundant work and types of deformation in extrusion-forging. Figure 5.6 represents a case of increased friction at container wall, as shown by severe distortion of the grid pattern in the corners of the die to produce a dead zone of segment which undergoes little deformation. Grid pattern at the centre of the billet sustain/experience essentially pure elongation in to the extruded rod, while elements near the sides of the billet defer extensive shear deformation. This shear distortion requires a consumption of energy which is not related to the change in external dimension from billet to extruded-forging product (this work



(a) Square-hexagon socket adapter

(b) Hexagon-hexagon socket adapter



(c) Square-square socket adopter

(d) Hexagon-square socket adopter

Figure 5.5 Metal flow patterns at different punch movement

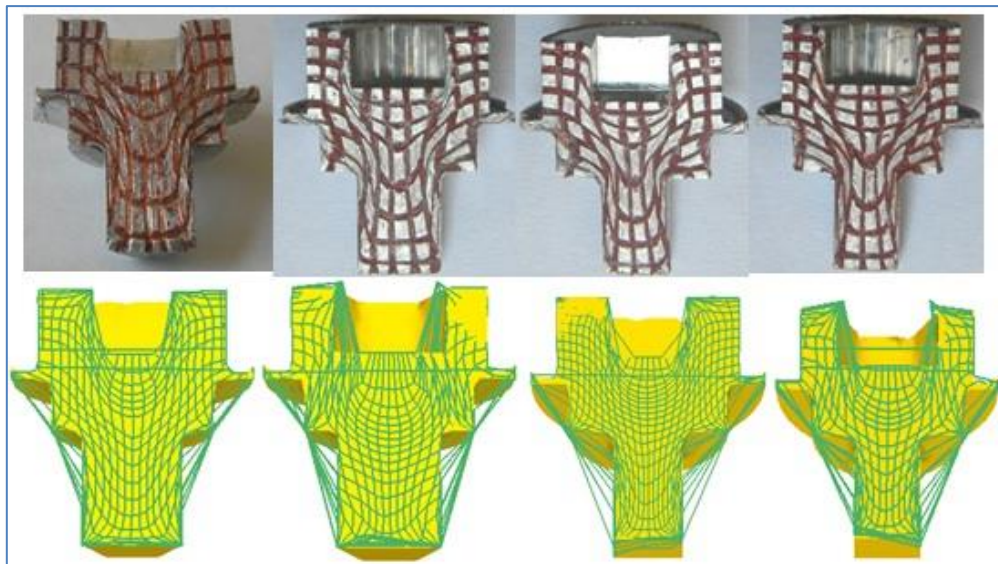


Figure 5.6 Full photographic views of patterns of metal deformation in extrusion-forging (the way of metal flows in the container indicates that, the required pressure for extrusion-forging process. Metal flow is concentrated toward the centre because of high friction at the die wall-billet interface).

5.1.4 Variation of Socket depth and extruded length

Here the socket depth increases up to the final dimension 5mm. Similarly the extruded length varies up to its final dimension 13mm (Figure 5.7). At the same time the socket depth and extruded length increase, this is indicating the metal flow for extrusion-forging. Pure

extrusion takes place after complete of the socket depth. Figure 5.8-5.11 illustrates the variation of socket depth and extruded length with punch travel for both of the experiment and simulation. Equal impression of punch head developed on billet in square-hexagon and square-square socket adopter with approximately same punch movement. And similar analysis for other two socket adopter. Initially nature of the extruded curve of different types of socket adopter shows the steady state extrusion; whereas nature of the curve towards the end indicates the forging. Middle portion of curve shows the combined extrusion forging.

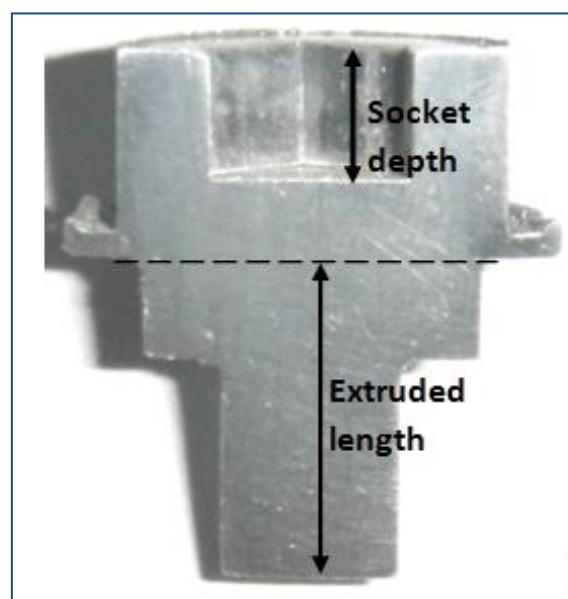


Figure 5.7 Socket depths and extruded length

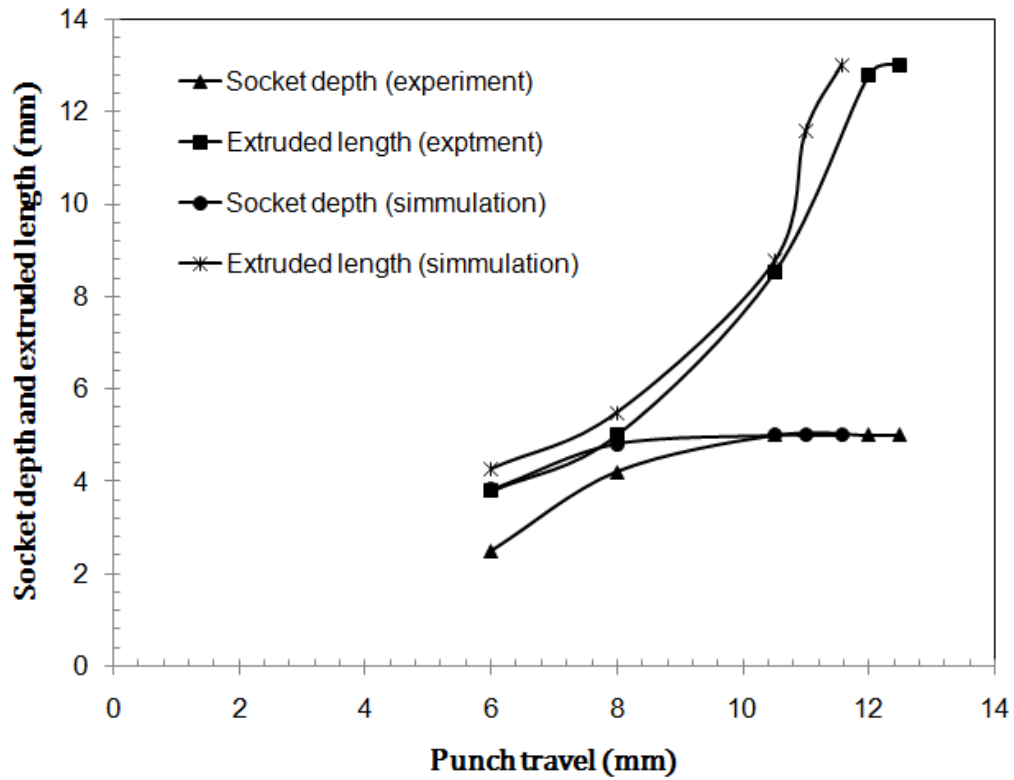


Figure 5.8 Variation of socket depth and extruded length for square-hexagon socket adopter

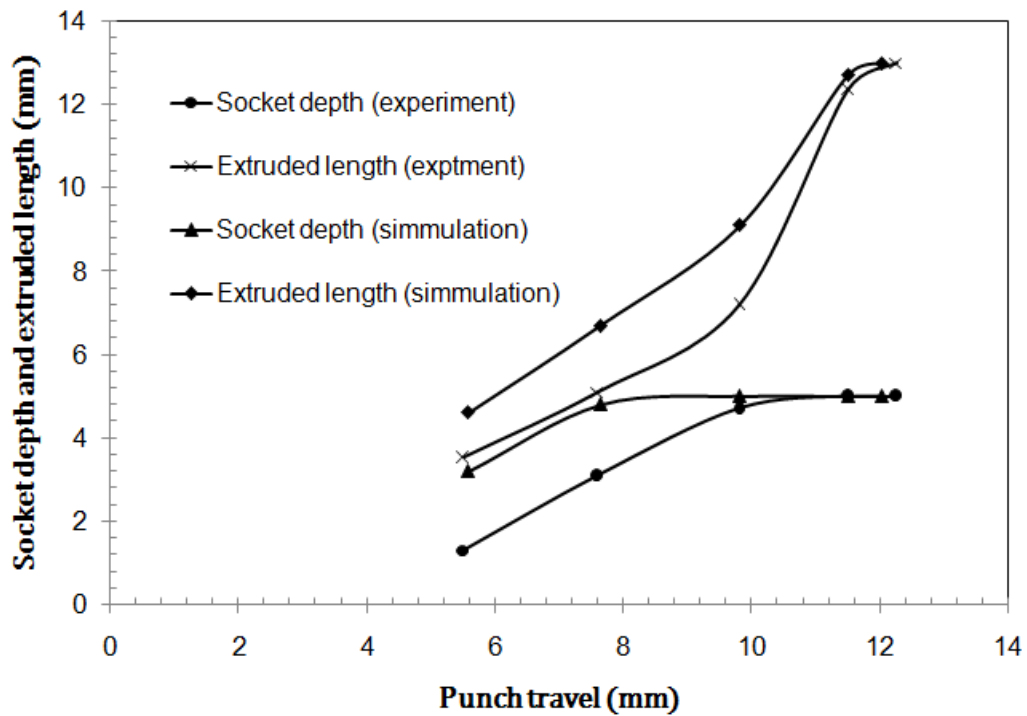


Figure 5.9 Variation of socket depth and extruded length for hexagon-hexagon socket adopter

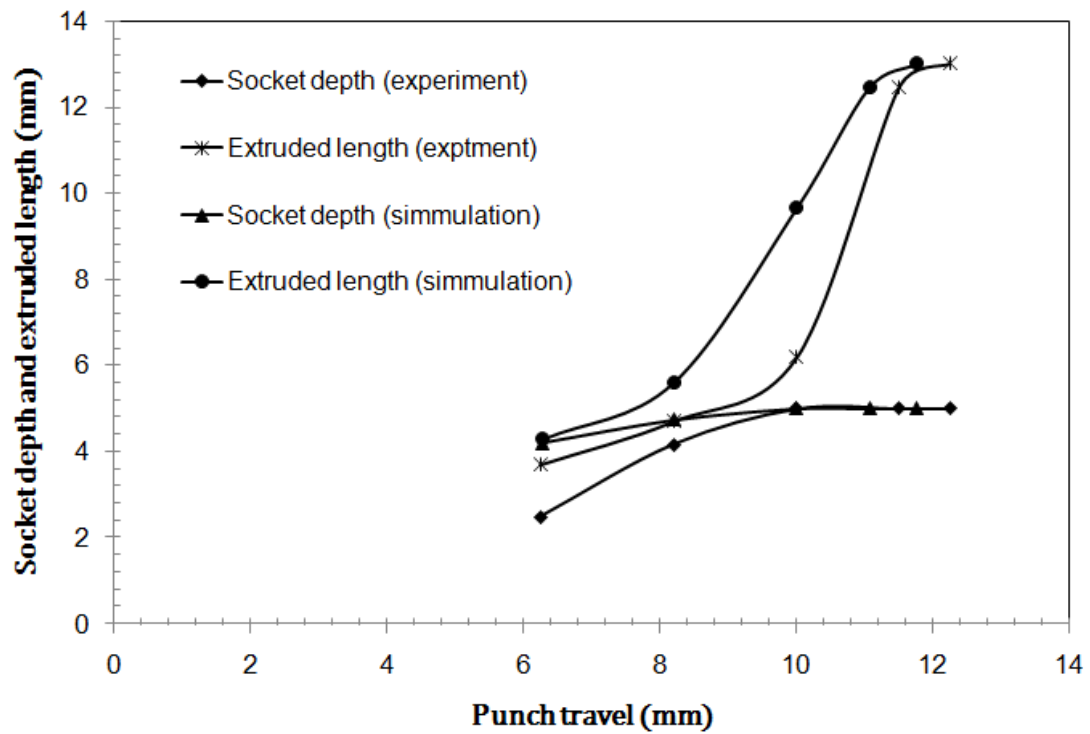


Figure 5.10 Variation of socket depth and extruded length for square-square socket adopter

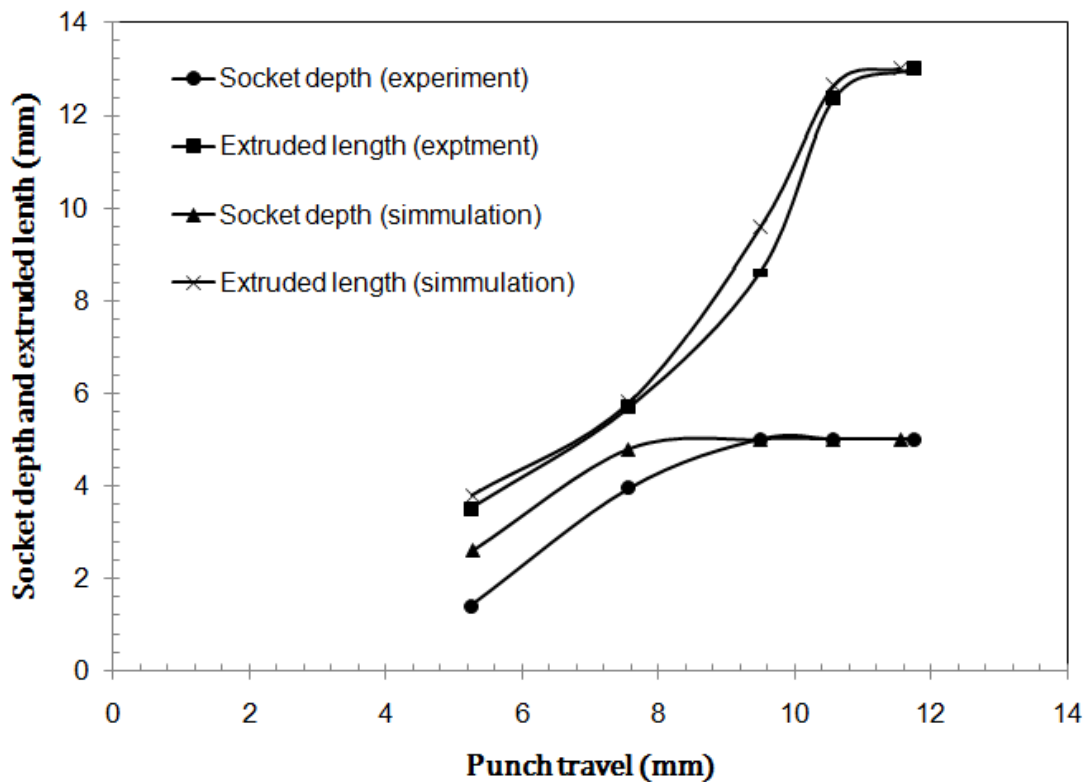


Figure 5.11 Variation of socket depth and extruded length for hexagon-square socket adopter

5.2 Conclusions

The experimental die filling, flow pattern and load requirements agree well with the FEM analysis. Socket depth and extruded length are simultaneously increases by movement of punch. This shows that the metal flow occurs both for forging and forward extrusion. The nature of metal flow grid lines are indicates that, the flow is homogeneous with friction at die-billet interface as well as container-billet interface.

CHAPTER 6

*CONCLUSIONS AND SCOPE
FOR FUTURE WORK*

6.1 Conclusions

The following conclusions are drawn from the present analysis:

- i. Finite element based Deform 3D simulation software was implemented successfully to analyze the effective stress, effective strain, stress mean, total velocity, load vs. punch displacement and metal flow pattern combined extrusion-forging process of aluminum rod with different die geometry, punch speed and friction factors.
- ii. A change in the die or punch alters the flow of metal and the pressure required to extrude a given product.
- iii. Total velocity flow for different extruded shapes are studied three dimensionally.
- iv. Punch displacement and maximum load of punch gives the idea to design the die and punch set up and simulating results will be useful during the execution of the experimental procedure and they will guide the experimental tests, which are going to take place in a real press with extrusion dies.
- v. Before going to the experiment, it is easy to visualize the extruded shape and flow pattern.
- vi. The obtained variation of punch load with respect to stroke by proposed technique is also well validated with FE analysis and experiment. It is also observed that with the increase of reduction variation of FE analysis with experimental results increases marginally with the addition of redundant work.
- vii. FEM based commercial package code is used for finite element analysis of the processes. The experimental die filling, flow pattern and load requirements agree well with the FEM analysis.
- viii. From hardness test it is concluded that at zone I, i.e along the centre line the micro hardness of metal is uniform. At zone II, micro hardness value decrease from centre

line to outward. It is because the strain hardening is less at out ward due the presence of dead metal zone. Hardness depends upon the effective strain.

- ix. Like metal flow pattern, the orientation of grains are occurred and change their shape after extrusion-forging process. Grain boundary changes during this process were closely related to plastic strain.
- x. Socket depth and extruded length are simultaneously increases by movement of punch. This shows that the metal flow occurs both for forging and forward extrusion.

6.2 Scope for future work

The present work will inspire the future investigators and have a wide scope for to explore many aspects of combined extrusion-forging processes. Some recommendations for future research include:

- ❖ This method can be extended to analyse section extrusion-forging of other solid and hollow shapes.
- ❖ Experiment can extend to hot combined extrusion-forging process other materials.
- ❖ The analysis can be extended for the extrusion of sections through converging, curve dies and taper die.
- ❖ The proposed FEA can be applied to determination of die stress.
- ❖ The nature of metal flow grid lines are can be analysed numerically for homogeneous material.

REFERENCES

- [1] Fr. Sagemuller, "Cold impact extrusion of large formed parts", Wire, no. 95, p 2, 1968.
- [2] H.D. Feldmann, "Cold extrusion of steel", Markblatt 201, prepared for Beratungsstelle fure Stahlverwendung, Dusseldorf, 1977.
- [3] C. Misirli and Y. Can, "An experimental study and designing process by using CAD/CAE: In combined open die forging-extrusion process of different shaped geometries from aluminium alloy sample", International journal of Modern Manufacturing Technology, vol. 2, no. 1, pp. 5-60, 2010.
- [4] Farhoumand and R. Ebrahimi, "Analysis of forward-backward-radial extrusion process", Materials Design, vol. 30, pp. 2152-2157, 2009.
- [5] J. Vickery and J. Monaghan, "An upper-bound analysis of a forging-extrusion process", Journal of Materials Processing Technology, vol. 55, pp. 103-110, 1995.
- [6] R. Narayanasamy, K. Baskaran, S. Arunachalam, and D. Muralikrishna, "An experimental investigation on barrelling of aluminium alloy billets during extrusion forging using different lubricants", Materials & Design, vol. 29, no. 10, pp. 2076-2088, 2008.
- [7] H. E. You-feng, XIE Shui-sheng, Cheng Lie, Huang Guo-jie and F.U. Yao, "FEM simulation of aluminum extrusion process in porthole die with pockets", Transaction of Nonferrous Metals Society of China, vol. 20, pp. 1067-1071, 2010.
- [8] C. MacCormack, J. Monaghan, "2D and 3D finite element analysis of a three stage forging sequence", Journal of Material Processing and Technology, vol. 127, pp. 48-56, 2002.

- [9] G. Fang, J. Zhou, J. Duszczek, "Extrusion of 7075 aluminium alloy through double-pocket dies to manufacture a complex profile", *Journal of material Processing Technology*, vol. 209, pp. 3050-3059, 2009.
- [10] R. K. Uyyuru, H. Valberg, "Physical and Numerical Analysis of the metal flow over the punch head in backward cup extrusion of Aluminium", *Journal of Material Processing and Technology*, vol. 172, pp. 312-318, 2006.
- [11] M. Ketabchi, H. Mohammadi, M. Izadi, "Finite-Element Simulation and Experimental Investigation of Isothermal backward Extrusion of 7075 Al alloy", *Arabian Journal for Science and Engineering*, vol. 37, no. 8, pp-2287-2296, 2012.
- [12] M. A. Zaeem, H. Alihosseini, K Dehghani and H. A. Shivaee, "Producing Ultra-fine grained aluminium rods by Cyclic forward-backward extrusion: Study of microstructure and mechanical properties", *Material Letters*, vol. 74, pp. 147-150, 2012.
- [13] S. A. Sadough, M. R. Rahmani, and V. Paouyafar, "Rheological behaviour microstructure and hardness of A356 Al alloy in semisolid state using backward extrusion process", *Transaction of Nonferrous Metals Society of China*, vol. 20, pp. s906-s910, 2010.
- [14] S. Y. Lin and F. C. Lin, "Radius ratio estimation and fold situation prediction of deformation on profile in forging extrusion process", *Computers and structures*, vol. 80, pp. 1817-1826, 2002.
- [15] M. M. Moshksar and R. Ebrahimi, "An analytical approach for backward-extrusion forging of regular polygonal hollow component", *International Journal of Mechanical Science*, vol.40, no.12, pp. 1247-1263, 1998.

- [16] C. Giarlini, E. Ceretti and G. Maccarini, “Formability in Extrusion forging: the influence of die geometry and friction condition”, *Journal of materials processing Technology*, vol. 54, pp. 302-308, 1995.
- [17] L. Brayden and J. Monaghan, “An analysis of closed-die extrusion/forging,” *Journal of Materials Processing Technology*, vol. 26, no. 2, pp. 141-157, Jun. 1991.
- [18] H. I. Lee, B. C. Hwang, and W. B. Bae, “A UBET analysis of non-axisymmetric forward and backward extrusion,” *Journal of Materials Processing Technology*, vol. 113, pp. 103-108, Jun. 2001.
- [19] H. Yamin, L. Zhouyi, and Z. Yucheng, “The study of cup-rod combined extrusion processes of magnesium alloy (AZ61A),” *Journal of Materials Processing Technology*, vol. 187-188, pp. 649-652, 2007.
- [20] G.-C. Wang, G.-Q. Zhao, X.-H. Huang and Y.-X. Jia, “ Analysis and design of a new manufacturing process for a support shaft using the finite element method”, *Journal of Materials Processing Technology*, vol. 121, pp. 259–264, 2002.
- [21] L. N. Patra and S. K. Sahoo, “3D analysis of extrusion-forging process: Pentagonal head with round shaft”, *International Journal of Applied Engineering*, vol. 1, pp. 2-8, 2011
- [22] L. N. Patra, S. K. Sahoo, and K. P. Maity, “Plastic Flow of Metal through Flat Dies: A Three Dimensional Analysis”, *International Journal of Mechanical and Materials Engineering*, vol. 1(3), pp. 160-165, 2010.
- [23] S. Z. Qamar, “Shape Complexity, Metal Flow, and Dead Metal Zone in Cold Extrusion”, *Materials and Manufacturing Processes*, vol. 25, pp. 1454–1461, 2010.
- [24] S. H. Kim, S. W. Chung and S. Padmanaban, “Investigation of lubrication effect on the backward extrusion of thin-walled rectangular aluminum case with large aspect ratio”, *Journal of Materials Processing Technology*, vol. 180, pp. 185–192, 2006.

- [25] A. Alfozan and J. S. Gunasekera, “An upper bound elemental technique approach to the process design of axisymmetric forging by forward and backward simulation”, *Journal of Materials Processing Technology*, vol. 142, pp. 619–627, 2003.
- [26] B. C. Hwang, S. J. Hong and W. B. Bae, “An UBET analysis of the non-axisymmetric extrusion/forging”, *Journal of Material Processing Technology*, vol. 111, pp. 135-141, 2001.
- [27] H. Y. Cho, G.S. Min, C. Y. Jo and Myung Han Kim, “Process design of the cold forging of a billet by forward and backward extrusion”, *Journal of Materials Processing Technology*, vol. 135, pp. 375–381, 2003.
- [28] M. S. J. Hashmi and F. B. Klemz, “Axisymmetric extrusion forging: effects of material property and product geometry”, *International Journal of Machine Tool Design Research*, vol.26, pp. 157–170, 1986.
- [29] W. Hu, M.S.J. Hashmi, “Study of metal flow in extrusion forging of rectangular billets”, *Journal of Material Processing Technology*, vol. 43, pp. 51–59.1994.
- [30] C. Giardini, E. Ceretti, G. Maccarini, “Formability in extrusion forging: the influence of die geometry and friction conditions, *Journal of Material Processing Technology*, vol. 54 pp. 302–308, 1995.
- [31] Chun-Yin Wu and Yuan-Chuan Hsu, “The influence of die shape on the flow deformation of extrusion forging”, *Journal of Materials Processing Technology*, vol. 124, pp. 67–76, 2002.
- [32] K. Kuzman, E. Pfeifer, N. Bay and J. Hunding, “Control of material flow in a combined backward can - forward rod extrusion”, *Journal of Materials Processing Technology*, vol. 60, pp. 141-147, 1996.
- [33] N. R. Chitkara and M. A. Bhutta, “Computer simulation to predict stresses, working pressures and deformation modes in near-net shape heading of a tapered circular bolt

- with a square head”, *International Journal of Machine Tools & Manufacture*, vol. 40, pp. 1849-1878, 2000.
- [34] N. R Chitkara and M. A Bhutta, “Forging and heading of hollow spur gear forms: an analysis and some experiments”, *International Journal of Mechanical Sciences*, vol. 41, pp. 1159-1189, 1999.
- [35] N. R. Chitkara and M. A. Bhutta, “Shape heading of splines and solid spur gear forms: an analysis and some experiments”, *International Journal of Mechanical Sciences* 43, pp. 1073-1106, 2001.
- [36] K. Kuzman, E. Pfeifer, N. Bay and J. Hunding, “Control of material flow in a combined backward can - forward rod extrusion”, *Journal of Materials Processing Technology*, vol. 60, pp. 141-147, 1996.
- [37] B. Bennani and N. Bay, “Limits of lubrication in backward can extrusion: analysis by the finite-element method and physical modelling experiments”, *Journal of Materials Processing Technology*, vol. 61, pp. 275-286, 1996.
- [38] S. I. OH, W. T. Wu, and J. P. Tang, “Simulation of Cold forging process by the DEFORM 3D system”, *Journal of Material Processing and Technology*, vol. 35, pp. 357-370, 1992.
- [39] M. Arentoft, P. Henningsen, N. Bay, and T. Wanheim, “Simulation of defects in metal forming-An example”, *Journal of Material Processing and Technology*, vol. 45, pp. 527-532, 1994.
- [40] H. Kim, K. Sweenery and T. Altan, “Application of computer aided simulation to investigated metal flow in selected forging operation”, *Journal of Material Processing and Technology*, vol. 46, pp. 127-154, 1994.
- [41] D. C. Chen, W. J. Chen, J. Y. Lin, M. W. Jheng, and J. M. Chen, “Finite element analysis of super plastic blow-forming of Ti-6Al-4V sheet into closed ellip-

cylindrical die”, International Journal of Simulation Modeling, vol. 9, no. 1, pp 17-27, 2010.

[42] G. Li, J. Yang, J. Y. Oh, M. Foster and W. Wu, “Advancements of Extrusion Simulation in DEFORM 3D”, Light Metal Age, Scientific Forming Tech. Corp. MIRDC, 2010

[43] T.G. Byerer, Forging Hand Book, American Society for Metals, ISBN: 0-87170-194-4.

COMMUNICATIONS

1. Kanhu Charan Nayak and Susant Kumar Sahoo, “Dynamic Simulation and Optimization of Extrusion Process for 2024 Aluminum Alloy”, Twenty-First International Symposium on Processing and Fabrication of Advance Materials, IIT Guwahati, India, Dec. 10-13, 2012.
2. Kanhu Charan Nayak and Susanta Kumar Sahoo, “Shaped Forging of Flywheel: A FEM Analysis” Third International Conference on Production and Industrial Engineering, NIT Jalandhar, India, March 29-31, 2013.